Mathematical and Computational Applications

MDPI

Article

Stochastic Analysis and Stability of Diabetic Population Dynamics

Jawaria [1], Guo Min [2], Jorge E. Macías-Díaz [3,4], Muhammad Waqas Yasin [5], Nauman Ahmed [6,7] and Luis E. Ayala-Hernández [8,9,*]

1 Department of Information and Communication Engineering (Complex Systems Modeling and Simulation), North University of China, Taiyuan 030051, China; jawariauog@gmail.com
2 School of Economics and Management, North University of China, Taiyuan 030051, China; guomin-like@sina.com.cn
3 Department of Mathematics and Physics, Autonomous University of Aguascalientes, Aguascalientes 20100, Aguascalientes, Mexico; jemacias@correo.uaa.mx or jorge.macias diaz@tlu.ee
4 Department of Mathematics and Didactics of Mathematics, Tallinn University, 10120 Tallinn, Estonia
5 Department of Mathematics, University of Narowal, Narowal 51600, Pakistan; waqasy286@gmail.com
6 Department of Mathematics and Statistics, The University of Lahore, Lahore 54000, Pakistan; nauman.ahmd01@gmail.com
7 Research Center of Applied Mathematics, Khazar University, Baku AZ1096, Azerbaijan
8 Departamento de Ciencias Exactas y Tecnología, Centro Universitario de los Lagos, Universidad de Guadalajara, Lagos de Moreno 47460, Jalisco, Mexico
9 Unidad Académica Lagos de Moreno, Instituto Tecnológico "José Mario Molina Pasquel y Henríquez", Tecnológico Nacional de México, Lagos de Moreno 47480, Jalisco, Mexico
* Correspondence: quique.a.h@hotmail.com or luis.ayala@lagos.tecmm.edu.mx

Abstract

Modeling diabetic illness with random perturbations is the goal of this work. The proposed model consists of three classes: the pre-diabetic population, the diabetic population with complications, and the diabetic population without complications. We examined the suggested problem to determine at least one unique solution within the positive feasible region. The stationary distribution of this model was also explored, and the non-negative C^2-Lyapunov function was used to create an adequate condition for the persistence of one stationary ergodic distribution. For this model, the existence and uniqueness of the solution were also established. Additionally, the stochastic non-standard finite difference (NSFD) scheme was developed for the model. The consistency and stability of the scheme were analyzed, showing that it is consistent and stable in the mean-square sense. The underlying system admits a unique endemic equilibrium point. Finally, a test problem was studied by using a numerical technique, varying the noise levels, and maintaining the same parameter values. The outcomes for each stated class were numerically simulated in order to validate our proposed approach.

Keywords: stochastic epidemic model; unique existence; stationary distribution

Check for updates

Academic Editors: Gianluigi Rozza and Alexandre Souto Martinez

Received: 3 July 2026
Revised: 8 September 2026
Accepted: 16 September 2026
Published: 22 September 2026

Copyright: © 2026 by the authors. Licensee MDPI, Basel, Switzerland. This article is an open access article distributed under the terms and conditions of the Creative Commons Attribution (CC BY) license.

1. Introduction

Diabetes is a chronic disease caused by a defect in the pancreatic mechanism that emits insulin in the body, which renders the cells incapable of taking glucose from the body for conventional utilization. Consequently, body sugar levels fluctuate and give rise to several problems and complications, like strokes, heart disease, amputation, and kidney disease. For diabetic patients, it is crucial to maintain the blood glucose level in their body in order to avoid such medical complications [1]. Regardless of age, gender, location, or region,

diabetes affects demographics worldwide and has been revealed as a major factor of both death and morbidity globally. Diabetes has two prevalent forms, Type 1 and Type 2. Type 1 diabetes is caused by the autoimmune destruction of the beta cells of the pancreas, and Type 2 diabetes is strongly associated with obesity; a sedentary, dull, and static lifestyle; and a substantial genetic component. Type 2 diabetes occurs globally and makes up approximately 90% of the 537 million diabetic cases, and this number is rapidly growing in children and young people up to age 40 [2]. Accordingly, Type 2 diabetes is a serious health issue in the U.S., affecting approximately 37.3 million young people. Additionally, approximately 98 million young people have pre-diabetes, a condition characterized by elevated blood glucose levels that are higher than normal, but do not meet the diagnostic criteria for diabetes [3].

Epidemiology uses real-world data to investigate a wide range of mathematical models of epidemics. Interest in epidemiology is increasing daily, which confirms the significance of the field. Previously, numerous mathematical models were developed, such as SI [4], SIR [5], SIS [6], SEIR [7], SARS [8], etc. All of these models were developed to offer real data-based predictions and to educate society and provide useful information about diseases, thereby contributing to improved public health and societal well-being [9]. Therefore, almost every biological disease or infection can be studied with a mathematical model, and an epidemiological framework can be established for these mathematical formulations [10]. Paliares et al. analyzed a Type 1 diabetes mellitus model for cardiovascular risk stratification in a multi-ethnic population and compared the results obtained from the Steno Type 1 Risk Engine (ST1RE) and the Scottish–Swedish risk model in young individuals with Type 1 diabetes [11]. Sibarani et al. developed a cardiovascular disease prediction model for the Indonesian adult population with pre-diabetes and diabetes mellitus and studied the Bogor Cohort of non-communicable disease risk factors. Almost 1085 patients with pre-diabetes and diabetes were included in this study, of whom approximately 73% were women. The authors concluded that young adults in Indonesia with pre-diabetes and diabetes are at risk of developing cardiovascular disease at age 45 or older within six years, highlighting the need for targeted intervention [12].

To research the general population and forecast the risk of Type 2 diabetes, Martínez-Hervás et al. [13] formulated a decision-based T2DM model that is entirely dependent on factors such as age, gender, body mass index (BMI), fasting plasma glucose (FPG), and fasting triglyceride (FTG) levels. About 93% of people were identified by this model, which also stated that T2DM will have a greater risk level in the upcoming year due to higher FPG levels in diabetic patients. If the FPG level is normal, age will determine the risk of T2DM, and BMI at the following levels. Furthermore, a diabetic patient has a higher chance of acquiring Type 2 diabetes if their FPG is lower and their FTG is higher. In addition, several researchers have developed a pre-diabetes and diabetes model with Type 1 and Type 2 in order to accurately estimate the risk of developing diabetes, raise public awareness about the importance of caring for people with diabetes, and present information and findings based on real-world data [14–17]. To diagnose diabetes, stochastic mathematical models of blood glucose dynamics were developed in the early stages of diabetes research [18,19]. Zhang et al. developed a stochastic second-order ordinary differential equation to explain how food consumption affects blood glucose levels using continuous monitoring (CGM) data devices. The proposed model represents a mechanistic framework with parameter values that vary between individuals with diabetes and healthy controls, and the authors discuss its implications for clinical practice [20].

A dairy nutrition epidemiology model was formulated by Slurink et al. [21]. The relationship between the baseline and the fluctuation in daily food consumption, the risk of pre-diabetes and diabetes, and the glycemic level was examined. The findings of this study,

therefore, showed that the majority of the foods and dairy products consumed in everyday life are not connected with the previously mentioned risk factors. Actually, daily use of high-fat foods, such as high-fat milk, is linked to an increased risk of pre-diabetes, which has to be investigated further to provide adequate data to support the findings. Therefore, in order to study and analyze how to overcome such chronic diseases with meaningful information and results, a dynamic model was developed to depict the uncertainties and treatments for pre-diabetes and diabetes related to many aspects [22–24]. Research on pre-diabetic and diabetic models with and without comorbidities is therefore advancing rapidly [25–27].

In addition to standard mathematical simulations, models developed by Boutayeb et al. have been analyzed to identify key risk factors for diabetes progression [28–30]. These factors typically fluctuate over time. Within this framework, a stochastic pre-diabetes and diabetes model was developed to estimate the risk intensity for pre-diabetic individuals and to forecast factor behavior. This model allows for early diabetes identification in pre-diabetic individuals by incorporating a random noise term into the model to capture individual variations in disease progression. It also provides valuable findings and insights into the dynamics of diabetes development, both with and without complications. The next section provides a detailed explanation of the mechanistic model based on established data [31]. To enhance the analysis, this model incorporates Brownian motion, which will be further elaborated upon in the subsequent section.

In this work, we propose a three-compartment stochastic differential equation model for diabetes dynamics that includes a clear progression pathway from pre-diabetes to serious complications. We establish threshold conditions for a unique ergodic stationary distribution and demonstrate the global existence, uniqueness, and positivity of solutions using a stochastic non-negative C^2 Lyapunov function. Furthermore, we formulate a nonstandard finite difference (NSFD) scheme to solve the system numerically and prove that it unconditionally preserves positivity. Our simulations show that the system performs better with the NSFD scheme than traditional Euler–Maruyama techniques, which yield non-physical negative solutions under extreme environmental noise.

Our work distinguishes itself from existing stochastic diabetes models in three key ways. First, our model captures rapid metabolic degradation under random environmental stress by incorporating a direct stochastic pathway from pre-diabetes to severe complications, in contrast to traditional models that only allow for sequential progression through compartments. Second, we rigorously verified the existence of a unique ergodic stationary distribution using a specially constructed logarithmic Lyapunov function customized to our three-dimensional coupled system, whereas previous research mostly relied on numerical simulations or simple threshold analyses. Third, we overcame a crucial drawback of standard Euler–Maruyama techniques, which frequently produce non-physical negative values under high volatility, by developing a nonstandard finite difference scheme that unconditionally preserves positivity regardless of step size. Together, these contributions offer more reliable computational tools and greater analytical insight into long-term disease dynamics.

The configuration of this paper is set up in the following manner. Section 2 provides a detailed introduction to the mechanistic population of pre-diabetic and diabetic models. This section also deduces the endemic equilibrium and the basic reproductive number $\bar{R}_0$. Then, the provided model is transformed into the stochastic OD model with a noise term, which also provides a detailed explanation of the model's stochastic significance. In Section 3, the main results are presented, such as the existence and uniqueness of the solution for the specified mechanistic model, followed by sufficient conditions for the ergodic stationary distribution $\bar{R}_1^T$ and disease persistence based on non-negative Lyapunov functions. This section also demonstrates the stochastic asymptotic behavior of the given

model at the endemic equilibrium point. Section 3.4 formulates the numerical approximation approaches, including the stochastic Euler–Maruyama (EM) and non-standard finite difference (NSFD) schemes along with their stability and a consistency analysis. Furthermore, Section 4 presents the graphical discussions, conclusions, and future research directions. Lastly, the complete mathematical proofs for the stationary distribution, stochastic stability analysis, and consistency analysis are detailed in Appendix A, Appendix B, and Appendix C, respectively.

2. The Proposed Model

This section includes the mathematical framework of the proposed three-compartmental diabetes model. First, we describe the population dynamics between pre-diabetic individuals $T(t)$, diabetic individuals without complications $U(t)$, and diabetic individuals with complications $V(t)$ under environmental fluctuations. Furthermore, we establish the theoretical connection between our compartmental structure, traditional SIR/SIRS epidemic frameworks, and stochastic resetting processes to record abrupt intervention shocks.

2.1. Mechanistic Population Diabetic Model

Boutayeb and Chetouani [31] introduced the three population segments in the mechanistic diabetes model based on the disease status. At time (t), the segments are described as $T(t)$ (number of pre-diabetic persons), $U(t)$ (number of diabetic persons without complications), and $V(t)$ (number of diabetic persons with complications). Furthermore, κ controls the recruitment of new pre-diabetic people into the community, while ϖ_1 represents the probability of the condition developing from pre-diabetes to complete diabetes. The complications that develop in diabetic patients are explained by the parameter ϖ_2, direct complications from the pre-diabetic stage itself are represented by $\varpi_3$number, θ models the natural death rate in all compartments, ζ permits recovery or reversal from the complications, ϑ handles the severe handicap brought on by these consequences, and ψ particularly monitors death directly related to diabetes complications.

$$\frac{dT(t)}{dt} = \kappa - (\theta + \varpi_3 + \varpi_1)T(t), \tag{1}$$

$$\frac{dU(t)}{dt} = \varpi_1 T(t) - (\theta + \varpi_2)U(t) + \zeta V(t), \tag{2}$$

$$\frac{dV(t)}{dt} = \varpi_3 T(t) + \varpi_2 U(t) - (\theta + \zeta + \vartheta + \psi)V(t). \tag{3}$$

Here, the total population $N(t)$ is $N(t) = T(t) + U(t) + V(t)$. By adding Systems (1)–(3), we formulated the following results:

$$\frac{dN(t)}{dt} = \kappa - \theta N(t) - (\vartheta + \psi)V(t). \tag{4}$$

When there are no diabetic patients, then the total population size will approach the carrying capacity $N(t) = \frac{\kappa}{\theta}$. The solution for the given model (1)–(3) will always be in range $\Xi_1 \in \Re^3_+$, which is defined as

$$\Xi_1 = \left\{ (T, U, V) | T \geq 0, U \geq 0, V \geq 0, T + U + V \leq \frac{\kappa}{\theta} \right\}.$$

If $\bar{R}_1^T > 1$ (see Theorem 2), then the given diabetic model (1)–(3) has only one equilibrium point, which is an endemic equilibrium point:

$$(T^*, U^*, V^*) = \left(\frac{\kappa}{(\theta+\omega_3+\omega_1)}, \frac{\kappa(\zeta\omega_3+\omega_1(\theta+\zeta+\vartheta+\psi))}{(\theta+\omega_3+\omega_1)(\theta(\theta+\zeta+\vartheta+\psi)+\omega_2(\theta+\vartheta+\psi))}, \frac{\kappa(\omega_1\omega_2+(\theta+\omega_2)\omega_3)}{(\theta+\omega_3+\omega_1)(\theta(\theta+\zeta+\vartheta+\psi)+\omega_2(\theta+\vartheta+\psi))} \right).$$

2.2. Stochastic Epidemic Model

Numerous health issues arise due to unaddressed factors such as limited healthcare control, unforeseen medical incidents, economic circumstances, and fluctuating lifestyle conditions. All these factors are uncertain and govern the results of diabetes management, disease progression, and diagnoses. One of the greatest benefits of a stochastic model is that these unpredictable variables can be modeled using stochastic terms, which provide longer, more realistic, and accurate predictions compared to deterministic models, which only provide average trends and flows. In actuality, the incidence rates or recovery rates might fluctuate from year to year or day to day, driving the uncertainty and randomness in the parameters. Deterministic models yield a single fixed forecast, whereas stochastic models have the capacity to capture the impact of these random occurrences while providing probabilistic predictions of the disease trajectory.

A stochastic model can assist in healthcare planning and resource allocation by generating probability distributions and evaluating extreme scenario outcomes. Stochastic simulations can mirror real empirical epidemiological data over time through a noise term that accounts for erratic fluctuations, rather than generating the smooth, idealized curves governed by deterministic models. A stochastic model also provides robust estimates for critical disease parameters, which can be utilized to enhance societal health criteria and mitigate disease risks. The formulation of stochastic differential equations (SDEs) is crucial across numerous fields, including epidemiology, engineering, and scientific applications.

Although transition and death rates are treated as fixed constants in deterministic models, real-world diabetes populations never exhibit such constancy. These presumed steady flows are constantly disrupted by everyday unpredictability, such as irregular eating patterns, abrupt lifestyle changes, uneven access to healthcare, and general environmental stresses. Stochastic differential equations embrace this complexity by modeling population trajectories as probability distributions rather than fixing the system to a single equilibrium point. This change is significant because it enables us to go beyond average behavior alone. We can now determine how much the outcomes generally fluctuate, estimate the probability of abrupt harmful spikes, and determine whether the illness burden is likely to continue or decline when real-world unpredictability is taken into account. Many researchers are now working to formulate the ODE into an SDE with the aim of addressing the noise term that predicts the uncertainty and randomness that influence the bulk of the applications. For detailed information on how one can formulate the ODE (1)–(3) into an SDE (5)–(7) by means of the Itô lemma, see [32–35]. Multitudinous researchers are now motivated to formulate the ODE into an SDE with the aim of addressing the noise term that predicts the uncertainty and randomness that influence the bulk of the applications. For detailed information on how one can formulate the ODE (1)–(3) into an SDE (5)–(7) by means of the Itô lemma, see [32–35].

By analyzing the stochastic formulations, scholars may investigate the random traumas in diabetic patients and determine whether diabetic patients are stable or facing instability combined with equilibrium points. A stochastic form of a system of SDEs is alternatively suggested by supplementing each equation with a product of diffusion coefficients ϱ_i and independent Brownian motion $\chi_i(t)$ $(i = 1, 2, 3)$, and hence, the stochastic model to the given mechanistic model (1)–(3) is shown below:

$$dT(t) = [\kappa - (\theta + \omega_3 + \omega_1)T(t)]dt + \varrho_1 T(t)d\chi_1, \tag{5}$$

$$dU(t) = [\omega_1 T(t) - (\theta + \omega_2)U(t) + \zeta V(t)]dt + \varrho_2 U(t)d\chi_2, \tag{6}$$

$$dV(t) = [\varpi_3 T(t) + \varpi_2 U(t) - (\theta + \zeta + \vartheta + \psi)V(t)]dt + \varrho_3 V(t) d\chi_3. \quad (7)$$

Here, χ_ι comprises standard Brownian motions and ϱ_ι comprises diffusion coefficients where $\iota = 1, 2, 3$. The standard Brownian motion χ_ι was chosen because it effectively models environmental noise in extensive populations, which embodies the aggregate effect of multiple separate, minor random disturbances. Furthermore, when the illness trajectory shows persistent temporal correlations or long-range memory effects, fractional Brownian motion may be used. If the diffusion coefficients $\varrho_1 = \varrho_2 = \varrho_3 = 0$, then the given model (5)–(7) will be a simplified model (1)–(3). The diffusion coefficients ϱ_1, ϱ_2, and ϱ_3 are represented by the standard Brownian motion, which demonstrates how strongly random environmental noise disturbs each compartment. From a biological perspective, they account for the natural day-to-day differences that cause real disease pathways to deviate from fixed deterministic predictions. These differences arise from changes in individual metabolism, shifting eating habits, varying stress levels, and unexpected environmental pressures. Larger diffusion coefficient values reflect greater uncertainty in the population progression rate, and this directly determines whether the system converges to a stable long-term pattern or faces a risk of extinction. These continuous random effects along a stochastic process can represent rapid changes to capture unexpected shocks such as policy actions or health care crises.

Connection to SIR/SIRS Frameworks and Stochastic Resetting

When transmission rates decline or the number of susceptible individuals decreases, the infection curve in standard SIR and SIRS models declines gradually. However, real-world public health events such as unexpected lockdowns, medical emergencies, or widespread screening initiatives cause sudden pauses in the transmission of illness that are difficult to account for with continuous Gaussian noise. A resetting stochastic process demonstrates these abrupt changes, in which the system abruptly returns to a fixed state at random intervals. Vinod et al. examined geometric Brownian motion with a resetting stochastic process and demonstrated how such random leaps alter the system's typical behavior and provide new long-term stable states [36]. Similarly, Wang et al. discovered that ergodicity can be restored in some diffusion processes by the diffusion process of stochastic resetting [37]. In our diabetes setting, a reset event could represent a nationwide lockdown that suddenly stops new pre-diabetic recruitment ($\kappa \to 0$) or a quick intervention that reduces complication rates ($\varpi_2 \to 0$). While our present work uses continuous standard Brownian noise to model everyday environmental variations, these reset frameworks offer a natural way to include sudden policy shocks in future work.

3. Main Results

3.1. Existence and Uniqueness

Theorem 1. *There exists a unique solution* $(T(t), U(t), V(t))$ *of the model (5)–(7)* $\forall \tau > 0$ *along with initial conditions* $(T(0), U(0), V(0)) \in \Re^3_+$. *Additionally, this unique solution will be in* $\Re^3_+$ *with probability* 1, *that is,* $((T(t), U(t), V(t)) \in \Re^3_+$ *for* $\forall \tau \geq 0$ *almost surely (a.s.) [38].*

Proof. A unique solution $(T(t), U(t), V(t)) \in \Re^3_+$ on $\tau[0, \Phi_e)$ should be exist on account of the local Lipschitz continuity of the coefficients in the model with regards to any initial conditions $(T(0), U(0), V(0)) \in \Re^3_+$. Adjacently, we have to prove this unique solution globally, i.e., $\Phi_e = \infty$. Suppose that all initial conditions lie in $[\frac{1}{\Upsilon_0}, \Upsilon_0] \times [\frac{1}{\Upsilon_0}, \Upsilon_0] \times [\frac{1}{\Upsilon_0}, \Upsilon_0]]$. Here, $\Upsilon_0 \geq$ is large enough. We define the time $\forall \Upsilon \geq \Upsilon_0$,

$$\Phi_\Upsilon = \inf \left\{ t \in [0, \Phi_e) : \max \{T(t), U(t), V(t)\} \geq \Upsilon \text{ or } \min \{T(t), U(t), V(t)\} \leq \frac{1}{\Upsilon} \right\}. \quad (8)$$

By convention, $\inf \varnothing = \infty$, where $\varnothing$ denotes the empty set. By the above definition of Φ_{Υ} (8), we can observe that Φ_{Υ} increases as $\Upsilon \to \infty$. Further, this establishes $\Phi_{\infty} = \lim_{\Upsilon \to \infty} \Phi_{\Upsilon}$ along with $\Phi_{\infty} \leq \Phi_e$ (a.s.). To prove that $\Phi_{\infty} = \infty$ (a.s.), we have to assume that $\Phi_e = \infty$, and hence, $(T(t), U(t), V(t))$ will be in $\Re^3_+$ (a.s.) for $\forall t \geq 0$. This condition is enough to prove that $\Phi_e = \infty$ (a.s.); if there is a contradiction, then there exists two constants $\omega, \top$ such that

$$\wp\left\{\Phi_{\infty} \leq \top\right\} > \omega.$$

Here, $\omega \in (0,1)$ and $\top > 0$ is defined as

$$\wp\left\{\Phi_{\Upsilon} \leq \top\right\} > \omega, \ \forall \Upsilon \geq \Upsilon_1. \tag{9}$$

Now, we define a C^2-Lyapunov function $\aleph : \Re^3_+ \to \Re_+$ by

$$\aleph(T, U, V) = (T - \log T - 1) + (U - \log U - 1) + (V - \log V - 1). \tag{10}$$

From conditions $p - \log p - 1 \geq 0$ and $\forall p > 0$, we observe that $\aleph$ is a non-negative function. Let $\forall \Pi \geq \Upsilon_0$ and $\forall \top > 0$; then, by Itô Lemma, we formulate the following result:

$$d\aleph(T, U, V) = Ł\aleph dt + \varrho_1(T-1)d\chi_1(t) + \varrho_2(U-1)d\chi_2(t) + \varrho_3(V-1)d\chi_3(t), \tag{11}$$

here, $Ł\aleph : \Re^3_+ \to \Re_+$ is defined below:

$$\begin{aligned} Ł\aleph &= \left(1 - \frac{1}{T}\right)dT + \frac{\varrho_1^2}{2} \\ &+ \left(1 - \frac{1}{U}\right)dU + \frac{\varrho_2^2}{2} \\ &+ \left(1 - \frac{1}{V}\right)dV + \frac{\varrho_3^2}{2} \end{aligned}$$

$$\begin{aligned} Ł\aleph &= \left(1 - \frac{1}{T}\right)\left[\kappa - (\theta + \varpi_3 + \varpi_1)T(t)\right] + \frac{\varrho_1^2}{2} \\ &+ \left(1 - \frac{1}{U}\right)\left[\varpi_1 T(t) - (\theta + \varpi_2)U(t) + \zeta V(t)\right] + \frac{\varrho_2^2}{2} \\ &+ \left(1 - \frac{1}{V}\right)\left[\varpi_3 T(t) + \varpi_2 U(t) - (\theta + \zeta + \vartheta + \psi)V(t)\right] + \frac{\varrho_3^2}{2} \end{aligned}$$

$$\begin{aligned} Ł\aleph &= \kappa + 3\theta + \varpi_1 + \varpi_2 + \varpi_3 + \zeta + \vartheta + \psi + \frac{\varrho_1^2 + \varrho_2^2 + \varrho_3^2}{2} \\ &- \left(\theta(T + U + V) + \vartheta V + \psi V + \frac{\kappa}{T} + \frac{\varpi_1 T}{U} + \frac{\zeta V}{U} + \frac{\varpi_3 T}{V} + \frac{\varpi_2 U}{V}\right). \end{aligned} \tag{12}$$

Since all state variables $T(t), U(t), V(t)$ and system parameters are strictly positive in $\Re^3_+$, the expression in the bracket under the negative sign is strictly positive. Therefore, eliminating this term provides the following upper bound:

$$Ł\aleph \leq \kappa + 3\theta + \varpi_1 + \varpi_2 + \varpi_3 + \zeta + \vartheta + \psi + \frac{\varrho_1^2 + \varrho_2^2 + \varrho_3^2}{2} := \Pi. \tag{13}$$

Integrating both sides of (11) from 0 to $\Phi_Y \wedge \top$ yields

$$\int_0^{\Phi_Y \wedge \top} d\aleph\Big(T(s), U(s), V(s)\Big) \leq \int_0^{\Phi_Y \wedge \top} \Pi ds + \int_0^{\Phi_Y \wedge \top} \Big[\varrho_1(T-1)d\chi_1(s) + \varrho_2(U-1)d\chi_2(s) + \varrho_3(V-1)d\chi_3(s)\Big].$$

Hence,

$$\begin{aligned} E\Big[\aleph(T(\Phi_Y \wedge \top), U(\Phi_Y \wedge \top), V(\Phi_Y \wedge \top))\Big] &\leq E\Big[\int_0^{\Phi_Y \wedge \top} \Pi ds\Big] + \aleph(T(0), U(0), V(0)) \\ &\leq \Pi\top + \aleph(T(0), U(0), V(0)), \end{aligned} \tag{14}$$

where $\Phi_Y \wedge \top = \min(\Phi_Y, \omega)$. Suppose $\Psi_Y = \{\Phi_Y \leq \top\}$ for $Y_1 \leq Y$ and $\omega \leq \wp(\Psi)$. For $\forall \eta \in \Psi_Y$, there exists at least one $T(\Phi_Y, \eta), U(\Phi_Y, \eta), V(\Phi_Y, \eta)$ that is equal to Y or $\frac{1}{Y}$. Therefore,

$$\aleph\Big((\Phi_Y, \eta), U(\Phi_Y, \eta), V(\Phi_Y, \eta)\Big) < \min\Big(Y - 1 - \log Y, \frac{1}{Y} - 1 + \log Y\Big)$$

$$\aleph\Big(T(\Phi_Y, \eta), U(\Phi_Y, \eta), V(\Phi_Y, \eta)\Big) \geq \Big(Y - 1 - \log Y\Big) \wedge \Big(\frac{1}{Y} - 1 + \log Y\Big).$$

According to (9) and (14), we formulate

$$\begin{aligned} \Pi\top + \aleph(T(0), U(0), V(0)) &\geq E\Big[1_\Phi(\eta)\aleph\Big(T(\Phi_Y, \eta), U(\Phi_Y, \eta), V(\Phi_Y, \eta)\Big)\Big] \\ &\geq \Big[\omega\Big(Y - 1 - \log Y\Big) \wedge \Big(\frac{1}{Y} - 1 + \log Y\Big)\Big], \end{aligned} \tag{15}$$

where $1_\Phi(\eta)$ denotes the indicator function of Φ. If we assume that $Y \to \infty$ gives rise to the contradiction $\infty = \aleph(T(0), U(0), V(0)) + \Pi\top < \infty$, then we have $\Phi_Y = \infty$ (a.s.). □

Remark 1. *The preceding Theorem 1 proves that the solution of the model (5)–(7) is globally positive and unique. While local Lipschitz continuity and stopping-time procedures are standard tools in stochastic analyses, applying them to this model requires constructing specialized bounding functions capable of controlling non-linear cross-coupled terms such as $\varpi_3 T(t)$ and $\zeta V(t)$. The mathematical novelty lies in constructing a C^2 global Lyapunov function that prevents the blow-up time τ_e from occurring in finite time ($\tau_e = \infty$ almost surely), thereby proving that the positive state space $\mathbb{R}^3_+$ is strictly invariant under coupled stochastic drift and diffusion operators.*

3.2. Stationary Distribution

The condition of the stationary distribution of this diabetic disease model is examined in the following section. For convenience, assume that [39]:

$$\langle Y(t) \rangle = \frac{1}{t}\int_0^t Y(z)dz.$$

To establish the condition for the stationary distribution, the subsequent Lemma 1 must be utilized.

Lemma 1. *Assume that $Y(t)$ is a regular Markov process (RMP) in $\Re_+^n$ whose dynamics are given by*

$$dY(t) = a(Y)dt + \sum_{r=1}^{n} f_z(Y)d\chi_z(t)$$

The diffusion matrix $Q(t)$ can be described as

$$Q(t) = (q_{lm}(y)), q_{lm}(y) = \sum_{r=1}^{n} f_z^l(y) f_z^l(y).$$

The RMP $Y(t)$ has a unique ergodic stationary distribution $\pi(.)$ if $\exists I \subset \Re_d$ is a bounded domain along the regular boundary λ and (i) there exists $S > 0$ such that $\sum_{l,m=1}^{3} q_{lm}(y)\alpha_l\alpha_m \geq S|\alpha|^2, \alpha \in \Re_d$. (ii) If there exist a non-negative C^2-Lyapunov function $\aleph^*$ such that $\Gamma\aleph^* < 0$ for any $\Re^d \backslash I$, then

$$M = \left\{ \lim_{\top\to\infty} \frac{1}{\top} \int_0^{\top} G(Y_y(t))dt = \int_{\Re^d} G(y)\pi(dy) \right\} = 1.$$

$\forall y \in \Re^d$, where $G(.)$ is an integrable function w.r.t. the measure π.

Theorem 2 ([38,40]). *The solution $(T(t), U(t), V(t))$ of (5)–(7) is ergodic and there is a unique stationary distribution $\pi(.)$ whenever*

$$\bar{R}_1^T = \frac{\varpi_1\kappa}{U_{max}(\theta + \varpi_3 + \varpi_1 + \frac{\varrho_1^2}{2})(\theta + \varpi_2 + \frac{\varrho_2^2}{2})} > 1.$$

Proof. See Appendix A for the detailed proof. □

Remark 2. *In the preceding Theorem 2 via Lemma 1, we showed that the model (5)–(7) is ergodic and has one unique stationary distribution (π). Pre-diabetic and diabetic populations would settle at a single fixed equilibrium under a deterministic framework, which seldom reflects heterogeneity in the real world. Instead, our stochastic model predicts that these subpopulations will persist indefinitely while varying due to random environmental factors. This is useful from the standpoint of biological planning, as it enables medical professionals to determine the precise likelihood that cases of complications would unexpectedly exceed hospital capacity, enabling data-driven readiness rather than relying on a single static projection.*

3.3. Stochastically Asymptotic Behavior

Theorem 3. *The equilibrium solution (T^*, U^*, V^*) of the stochastic system (5)–(7) is stochastically asymptotically stable on I if*

$$\frac{1}{2}\varrho_1^2 T^* + \frac{n_1}{2}\varrho_2^2 U^* + \frac{n_2}{2}\varrho_3^2 V^* \leq \eta_4(T, U, V), \tag{16}$$

where $n_1, n_2 > 0$ and

$$\eta_4(T, U, V) = A_T(T, U, V)(T - T^*)^2 + A_U(T, U, V)(U - U^*)^2 + A_V(T, U, V)(V - V^*)^2,$$

with

$$A_T = \frac{\theta + \omega_1 + \omega_3}{T} - \frac{n_1\omega_1}{2U} - \frac{n_2\omega_2}{2V},$$
$$A_U = \frac{n_1(\theta + \omega_2)}{U} - \frac{n_1\omega_1}{2U} - \frac{1}{2}\left(\frac{n_1\zeta}{U} + \frac{n_2\omega_3}{V}\right),$$
$$A_V = \frac{n_2(\theta + \zeta + \vartheta + \psi)}{V} - \frac{1}{2}\left(\frac{n_1\zeta}{U} + \frac{n_2\omega_3}{V}\right) - \frac{n_2\omega_2}{2V}.$$

The positive constants n_1 and n_2 were selected so that $A_T > 0$, $A_U > 0$, and $A_V > 0$ on the compact domain I.

Proof. Construct a suitable non-negative C^2-Lyapunov function for the endemic equilibrium as follows:

$$\aleph(T, U, V) = \left(T - T^* - T^* \ln \frac{T}{T^*}\right) + n_1\left(U - U^* - U^* \ln \frac{U}{U^*}\right) + n_2\left(V - V^* - V^* \ln \frac{V}{V^*}\right). \tag{17}$$

Here, $n_1, n_2 > 0$ are constants. By applying the Itô lemma on $\aleph(T, U, V)$, System (5)–(7) is formulated as

$$\text{Ł}\aleph = \left(1 - \frac{T^*}{T}\right)\left(\kappa - (\theta + \omega_3 + \omega_1)T(t)\right) + n_1\left(1 - \frac{U^*}{U}\right)\left(\omega_1 T(t) - (\theta + \omega_2)U(t) + \zeta V(t)\right)$$
$$+ n_2\left(1 - \frac{V^*}{V}\right)\left(\omega_3 T(t) + \omega_2 U(t) - (\theta + \zeta + \vartheta + \psi)V(t)\right) + \frac{1}{2}\varrho_1^2 T^* + \frac{n_1}{2}\varrho_2^2 U^* + \frac{n_2}{2}\varrho_3^2 V^*.$$

Using the equilibrium relations, this becomes

$$\text{Ł}\aleph = -\frac{(\theta + \omega_1 + \omega_3)}{T}(T - T^*)^2 - \frac{n_1(\theta + \omega_2)}{U}(U - U^*)^2 - \frac{n_2(\theta + \zeta + \vartheta + \psi)}{V}(V - V^*)^2$$
$$+ \left(\frac{n_1\zeta}{U} + \frac{n_2\omega_3}{V}\right)(U - U^*)(V - V^*) + \frac{n_1\omega_1}{U}(U - U^*)(T - T^*) + \frac{n_2\omega_2}{V}(V - V^*)(T - T^*)$$
$$+ \frac{1}{2}\varrho_1^2 T^* + \frac{n_1}{2}\varrho_2^2 U^* + \frac{n_2}{2}\varrho_3^2 V^*.$$

Applying $2ab \leq a^2 + b^2$ to each mixed product gives

$$\text{Ł}\aleph \leq -A_T(T, U, V)(T - T^*)^2 - A_U(T, U, V)(U - U^*)^2$$
$$- A_V(T, U, V)(V - V^*)^2 + \frac{1}{2}\varrho_1^2 T^* + \frac{n_1}{2}\varrho_2^2 U^* + \frac{n_2}{2}\varrho_3^2 V^*.$$

Therefore,

$$\text{Ł}\aleph \leq -\eta_4(T, U, V) + \frac{1}{2}\varrho_1^2 T^* + \frac{n_1}{2}\varrho_2^2 U^* + \frac{n_2}{2}\varrho_3^2 V^*.$$

Under condition (16), $\text{Ł}\aleph \leq 0$ on I; hence, the Lyapunov function is non-increasing in the stochastic sense. Consequently, the equilibrium solution (T^*, U^*, V^*) of System (5)–(7) is stochastically asymptotically stable on I. □

3.4. Numerical Schemes and Simulations

3.4.1. Stochastic EM Numerical Scheme

The EM numerical scheme for the given model (5)–(7) is formulated as

$$T^{J+1} = T^J + \Delta\tau\left[\kappa - (\theta + \omega_1 + \omega_3)T^J\right] + \varrho_1 T^J\left(\chi_{1(J+1)\Delta\tau} - \chi_{1(J)\Delta\tau}\right), \tag{18}$$

$$U^{J+1} = U^J + \Delta\tau\left[\varpi_1 T^J - (\theta + \varpi_2)U^J + \zeta V^J\right] + \varrho_2 U^J\left(\chi_{2(J+1)\Delta\tau} - \chi_{2(J)\Delta\tau}\right), \tag{19}$$

$$V^{J+1} = V^J + \Delta\tau\left[\varpi_3 T^J + \varpi_2 U^J - (\theta + \zeta + \vartheta + \psi)V^J\right] + \varrho_3 V^J\left(\chi_{3(J+1)\Delta\tau} - \chi_{3(J)\Delta\tau}\right), \tag{20}$$

where $J = 0, 1, \ldots, 2000$, $\Delta\tau = 1$ day, and χ_1, χ_2, χ_3 are independent standard Wiener processes. Consequently, the increments $\chi_{i(J+1)\Delta\tau} - \chi_{i(J)\Delta\tau}$ are independent random variables for each $i = 1, 2, 3$.

3.4.2. Stochastic NSFD Numerical Scheme

The numerical approximation solution is formulated through numerous numerical methods. Standard numerical techniques, such as the Euler–Maruyama and Milstein methods, are used to approximate differential terms linearly. When applied to population dynamics governed by non-linear transition rates, these conventional schemes frequently produce non-physical negative population values ($T^J, U^J, V^J < 0$) and suffer from severe numerical instabilities unless the time step size Δt is kept infinitesimally small. In contrast, by employing non-local representations for non-linear terms, the proposed nonstandard finite difference (NSFD) scheme guarantees that the discrete state variables remain strictly positive ($T^J, U^J, V^J < 0$) unconditionally for any time step size $\Delta t > 0$. The NSFD numerical scheme for the given model (5)–(7) is formulated as [41]

$$T^{J+1} = \frac{T^J + \kappa\Delta\tau + \varrho_1 T^J(\chi_{1(J+1)\Delta\tau} - \chi_{1(J)\Delta\tau})}{1 + \Delta\tau(\theta + \varpi_3 + \varpi_1)}, \tag{21}$$

$$U^{J+1} = \frac{U^J + \Delta\tau(\varpi_1 T^J + \zeta V^J) + \varrho_2 U^J(\chi_{2(J+1)\Delta\tau} - \chi_{2(J)\Delta\tau})}{1 + \Delta\tau(\theta + \varpi_2)}, \tag{22}$$

$$V^{J+1} = \frac{V^J + \Delta\tau(\varpi_3 T^J + \varpi_2 U^J) + \varrho_3 V^J(\chi_{3(J+1)\Delta\tau} - \chi_{3(J)\Delta\tau})}{1 + \Delta\tau(\theta + \zeta + \vartheta + \psi)}. \tag{23}$$

3.5. Stability Analysis

Theorem 4. *The stochastic NSFD scheme for Equations (21)–(23) is stable along stochastic ODE Equations (5)–(7) in the mean square.*

Proof. See Appendix B for the detailed proof. □

3.6. Consistency Analysis

A stochastic NSFD scheme $\mathcal{L}|_{(J)}T|_{(J)} = F|_{(J)}$ is consistent point-wise with the SDE $\mathcal{L}T = F$ at a point t, for any function $\Omega(t) = \Omega$ that is continuously differentiable in mean square, that is [42]

$$E||(\mathcal{L}\Omega - F)|_{(J)} - [\mathcal{L}|_{(J)}\Omega|_{(J\Delta\tau)} - F_{(J)}]||^2 \to 0,$$

as $\Delta\tau \to \infty$ and $((J+1)\Delta\tau)$ approaches (t).

Theorem 5. *The stochastic NSFD scheme for Equations (21)–(23) is consistent along stochastic ODE Equations (5)–(7) in the mean square.*

Proof. The complete mathematical verification is provided in Appendix C. □

4. Discussion and Conclusions

4.1. Discussion

The given stochastic population of pre-diabetes and diabetes model is

$$dT(t) = [\kappa - (\theta + \varpi_3 + \varpi_1)T(t)]dt + \varrho_1 T(t)d\chi_1,$$

$$dU(t) = [\varpi_1 T(t) - (\theta + \varpi_2)U(t) + \zeta V(t)]dt + \varrho_2 U(t)d\chi_2,$$

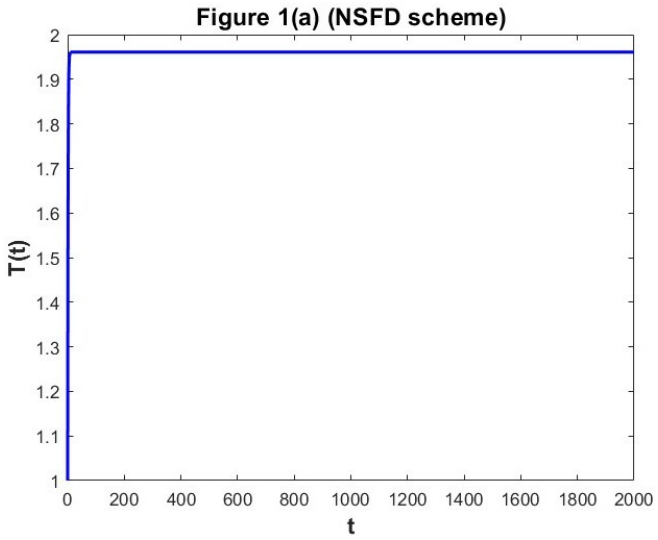
$$dV(t) = [\varpi_3 T(t) + \varpi_2 U(t) - (\theta + \zeta + \vartheta + \psi)V(t)]dt + \varrho_3 V(t)d\chi_3,$$

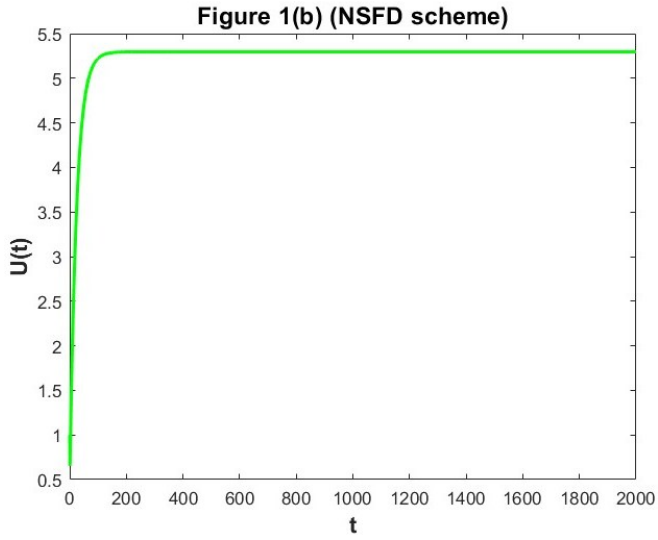
with initial conditions for $(T(t), U(t), V(t))$ of $T(1) = U(1) = V(1) = 1$ and an endemic equilibrium point for $(T(t), U(t), V(t))$:

$$(T^*, U^*, V^*) = \left(\frac{\kappa}{(\theta + \varpi_3 + \varpi_1)}, \frac{\kappa(\zeta\varpi_3 + \varpi_1(\theta + \zeta + \vartheta + \psi))}{(\theta + \varpi_3 + \varpi_1)(\theta(\theta + \zeta + \vartheta + \psi) + \varpi_2(\theta + \vartheta + \psi))}, \right.$$
$$\left. \frac{\kappa(\varpi_1\varpi_2 + (\theta + \varpi_2)\varpi_3)}{(\theta + \varpi_3 + \varpi_1)(\theta(\theta + \zeta + \vartheta + \psi) + \varpi_2(\theta + \vartheta + \psi))} \right) \quad (24)$$

Figures 1–3 are composed of the NSFD numerical scheme of $T(t)$, $U(t)$, $V(t)$ for the stochastic model (5)–(7) along with the values of parameters $\varpi_1 = 0.5, \varpi_2 = 2.5$, $\varpi_3 = 0.5, \kappa = 2, \theta = 0.02, \zeta = 0.8, \vartheta = 0.05, \psi = 0.01$, N = 30,000, $\Delta\tau = 1000/N$ [31], with noise $\varrho_i, i = 1, 2, 3$. Figure 1 demonstrates the behavior of the stochastic model with noise $\varrho_i = 0, i = 1, 2, 3$, which is also regarded as the mechanistic model of the formulated stochastic model. Figure 2 elaborates on the convergent behavior of the NSDF scheme for the stated stochastic model with noise $\varrho_i = 0.03, i = 1, 2, 3$ and the remaining parameter values unchanged. Likewise, Figure 3 exhibits the stochastic behavior of $(T(t), U(t), V(t)$ for the stochastic system at noise $\varrho_i = 0.06, i = 1, 2, 3$. Figure 4 displays the relationship between $\bar{R}_1^T$, κ and ϖ_2 for the stochastic model (5)–(7) at $\kappa = 5$ and $\varpi = 1.5$ with a contour plot of $\bar{R}_1^T$ and its corresponding 2D simulations of $T(t)$, $U(t)$, $V(t)$ for the stochastic scheme. In accordance with the above parameter values, we attained $\bar{R}_1^T \approx 1.4728 > 1$, which satisfied the condition for the persistence of the stationary distribution, and hence, Figure 4 demonstrates the stationary distribution criteria clearly. Eventually, we discovered that the stochastic NSDF numerical scheme converges to the endemic equilibrium point together with the dynamical existence and uniqueness, stochastic consistency, boundedness, and positivity, regardless of the time step size. In closing, we perceive that all figures validate the theoretical findings numerically.

Figure 5 is composed of the EM numerical scheme of $T(t)$, $U(t)$, $V(t)$ for the stochastic model (5)–(7) along with the values of parameters $\varpi_1 = 0.5, \varpi_2 = 2.5$, $\varpi_3 = 0.5$, $\kappa = 2, \theta = 0.02, \zeta = 0.8, \vartheta = 0.05, \psi = 0.01$, N = 30,000, $\Delta\tau = 1000/N$ [31], with noise $\varrho_i = 0.03, i = 1, 2, 3$, and it elaborates on the negative and non-convergent behavior of the EM scheme for the stated stochastic model. We used several step sizes and noise intensities to compare the suggested NSFD scheme with the conventional Euler–Maruyama approach. At bigger step sizes, such as $\Delta t = 1$, the EM technique produced non-physical negative values because the linear drift was overwhelmed by the stochastic increments. However, for every evaluated step size between $\Delta t = 0.01$ and $\Delta t = 2.0$, our NSFD approach maintained strict positivity in every compartment. Additionally, it maintained dynamic consistency with the continuous system, demonstrating its obvious practical benefit over traditional explicit solvers.





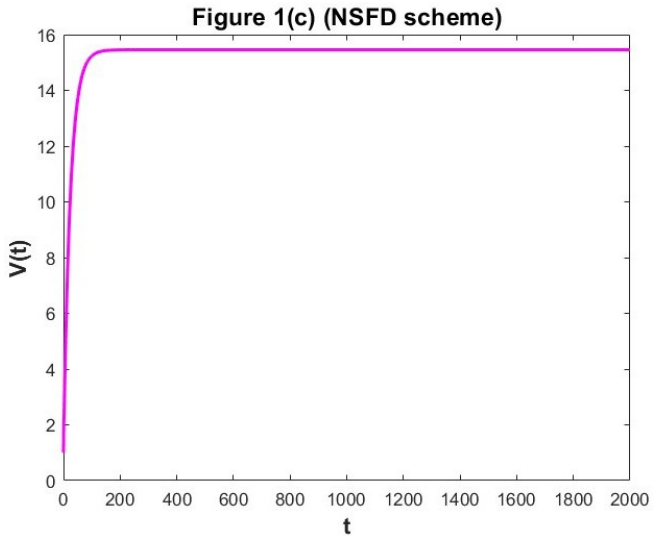


Figure 1. The 2D simulations of $T(t)$, $U(t)$, $V(t)$ for the NSFD numerical scheme of the stochastic model (5)–(7) along $\varpi_1 = 0.5, \varpi_2 = 2.5, \varpi_3 = 0.5, \kappa = 2, \theta = 0.02, \zeta = 0.8, \vartheta = 0.05, \psi = 0.05, \varrho_i = 0$, $i = 1, 2, 3$.

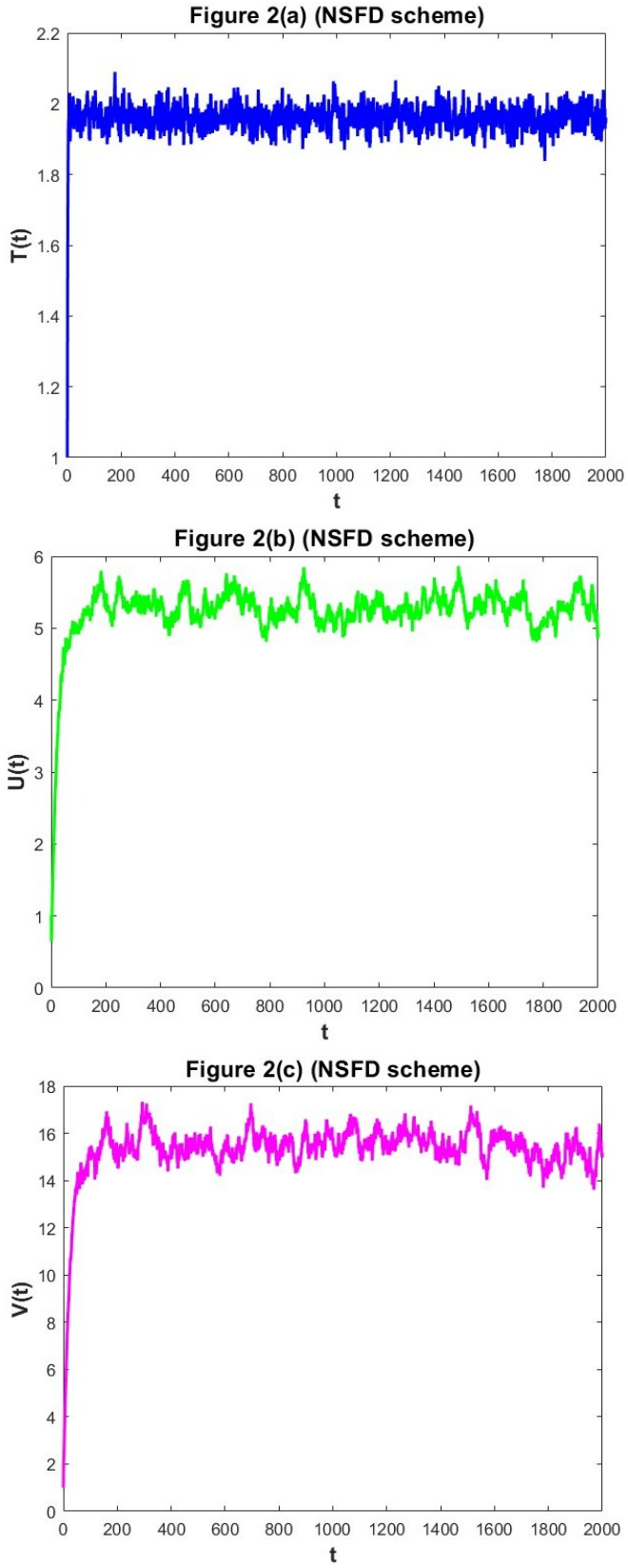


Figure 2. The 2D simulations of $T(t)$, $U(t)$, $V(t)$ for the NSFD numerical scheme of the stochastic model (5)–(7) along $\varpi_1 = 0.5, \varpi_2 = 2.5, \varpi_3 = 0.5, \kappa = 2, \theta = 0.02, \zeta = 0.8, \vartheta = 0.05, \psi = 0.05$, $\varrho_i = 0.03, i = 1, 2, 3$.

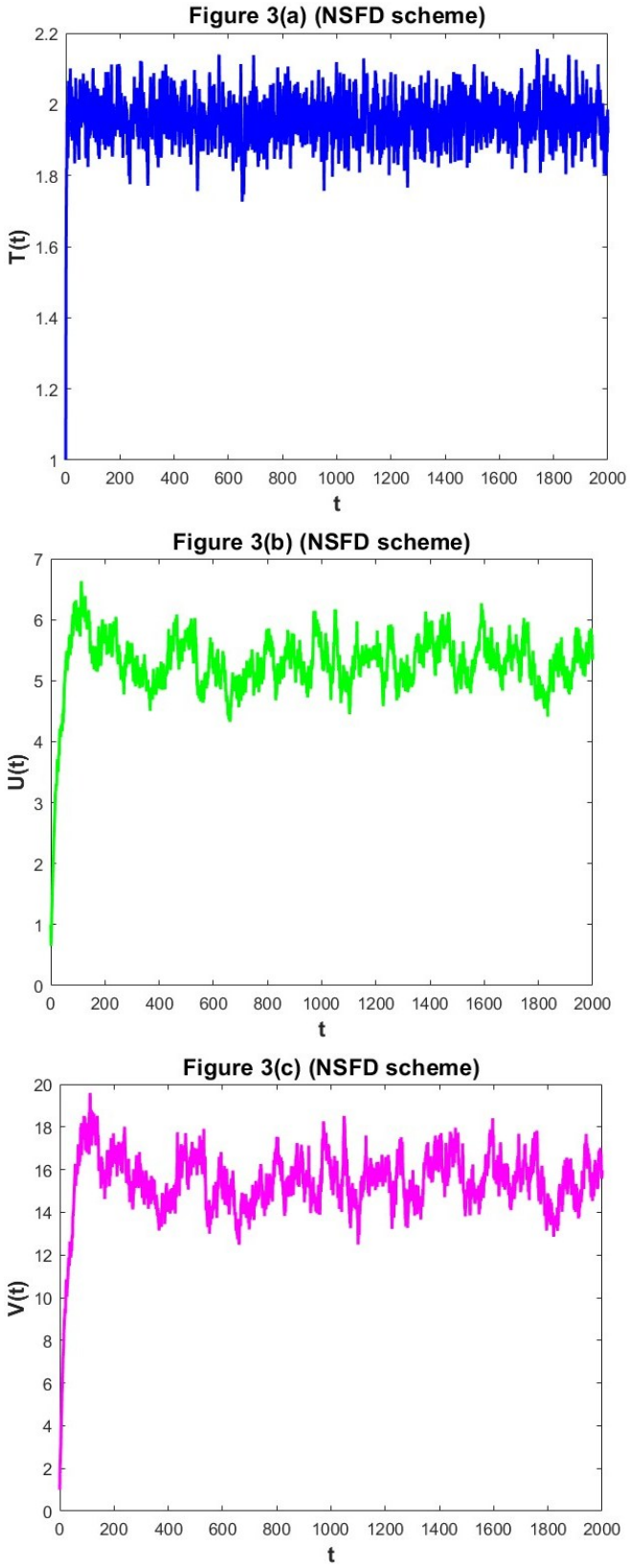


Figure 3. The 2D simulations of $T(t)$, $U(t)$, $V(t)$ for the NSFD numerical scheme of the stochastic model (5)–(7) along $\varpi_1 = 0.5, \varpi_2 = 2.5, \varpi_3 = 0.5, \kappa = 2, \theta = 0.02, \zeta = 0.8, \vartheta = 0.05, \psi = 0.05$, $\varrho_i = 0.06$, $i = 1, 2, 3$.

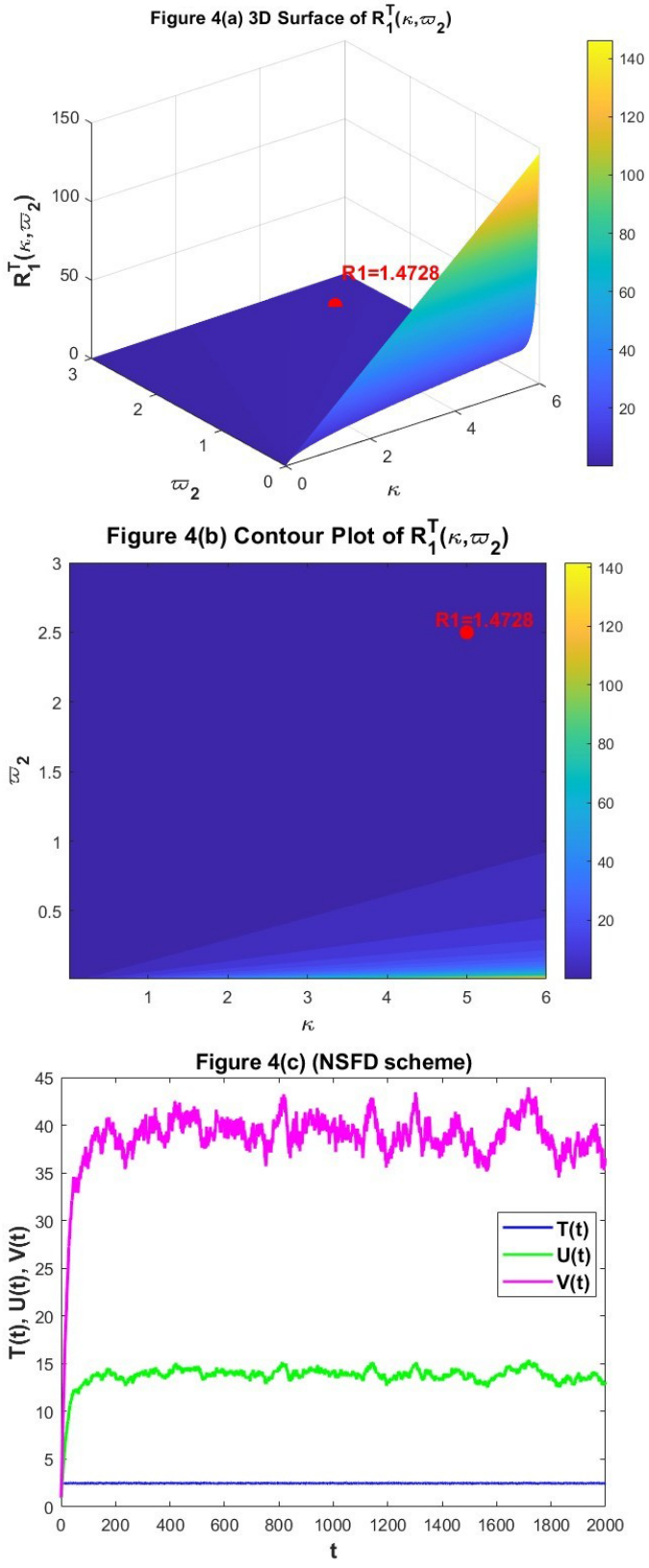


Figure 4. The relationship between $\bar{R}_1^T$, κ and ψ for the stochastic model (5)–(7) at $\kappa = 2$ and $\psi = 0.01$ with a contour plot of $\bar{R}_1^T$ and its corresponding 2D simulations of $T(t)$, $U(t)$, $V(t)$ for the stochastic scheme of model (5)–(7) $\bar{R}_1^T(\kappa,\psi)$ along $\varpi_1 = 1.5, \varpi_2 = 2.5, \varpi_3 = 0.5, \kappa = 5, \theta = 0.02, \zeta = 0.8$, $\vartheta = 0.05$, $\psi = 0.01, \varrho_i = 0.03$, $i = 1, 2, 3$.

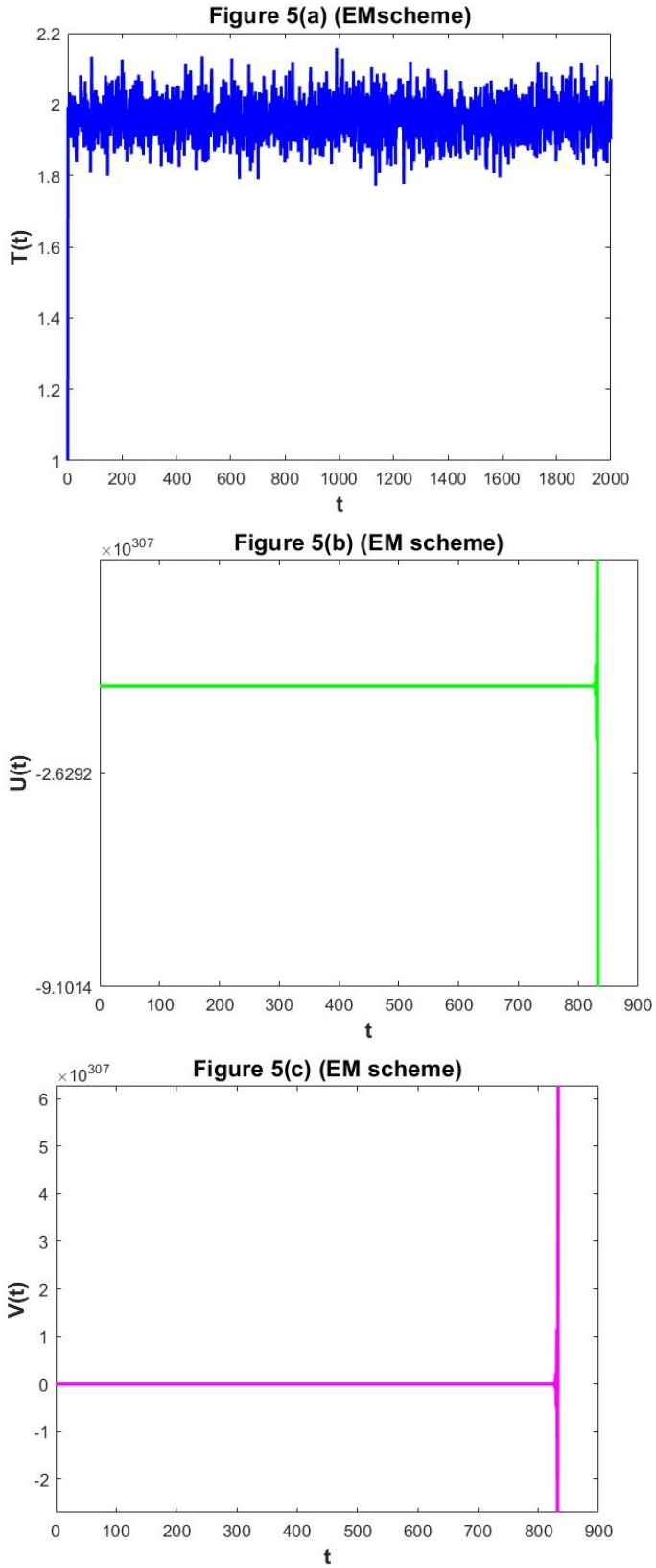
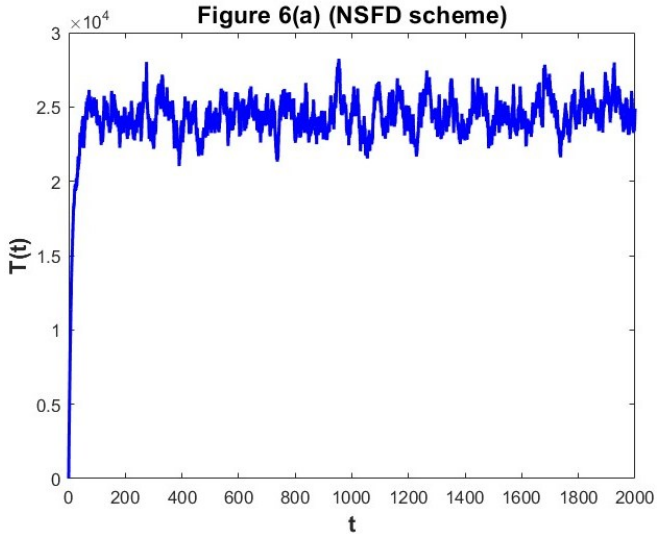


Figure 5. The 2D simulations of $T(t), U(t), V(t)$ for the EM numerical scheme of the stochastic model (5)–(7) along $\varpi_1 = 0.5, \varpi_2 = 2.5, \varpi_3 = 0.5, \kappa = 2, \theta = 0.02, \zeta = 0.8, \vartheta = 0.05, \psi = 0.01, \varrho_i = 0.03$, $i = 1, 2, 3$.

Figure 6 shows the behavior of the NSFD scheme of $T(t)$, $U(t)$, $V(t)$ for the stochastic model (5)–(7) along with real diabetic clinical data. The recruitment rate into the pre-diabetic compartment was taken as $\kappa = 2000$, the natural death rate was fixed at $\theta = 0.014$, and the extra death rate due to the disease was fixed as $\psi = 0.035$ [43]. The rate at which pre-diabetes progresses to uncomplicated diabetes was taken as $\varpi_1 = 0.060$, which is about 6% per year. This matches the clinical conversion standards given by [44]. For the transition from uncomplicated to complicated diabetes, we used $\varpi_2 = 0.040$, and the disability rate caused by complications was set at $\vartheta = 0.020$ [45]. The direct jump from pre-diabetes to severe complications was fixed as $\varpi_3 = 0.008$, based on findings from long-term cohort studies that track undiagnosed severe hyperglycemia [46]. Lastly, the recovery and stabilization rate was set at $\zeta = 0.035$ [47]. To include real-world randomness in the model, we set the stochastic noise intensities to $\varrho_i = 0.006, i = 1, 2, 3$. The whole system was then run for $t \in [0, 2000]$ days using a fixed step size of $\Delta\tau = 1$ day. Because every parameter was grounded in these trusted empirical sources, the simulated paths over the 2000 days should reflect the true population-level diabetes behavior of the proposed model.



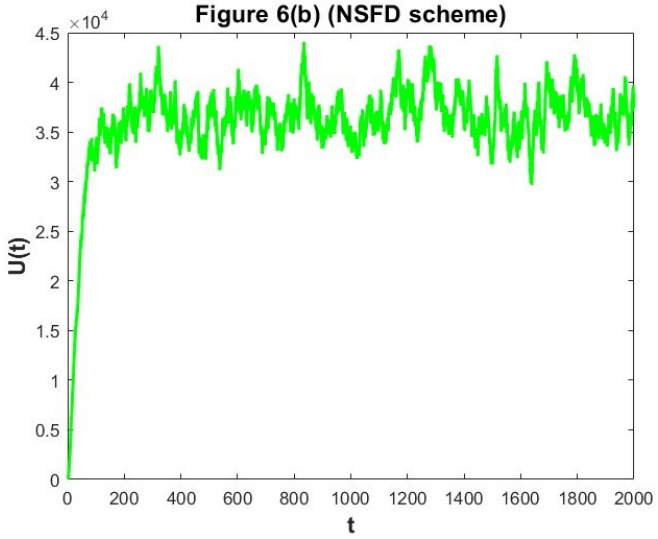


Figure 6. *Cont.*

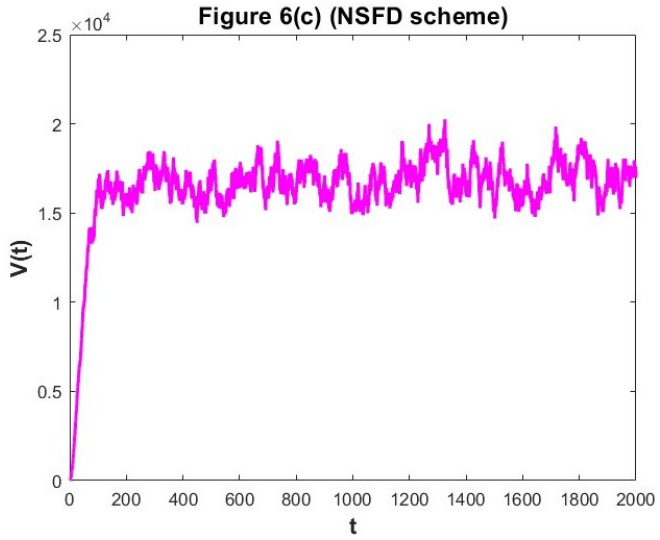


Figure 6. The 2D simulations of $T(t)$, $U(t)$, $V(t)$ for the NSFD numerical scheme of the stochastic model (5)–(7) along real data $\varpi_1 = 0.060, \varpi_2 = 0.040, \varpi_3 = 0.008, \kappa = 2000, \theta = 0.014, \zeta = 0.8$, $\vartheta = 0.020, \psi = 0.035, \varrho_i = 0.006, i = 1, 2, 3$.

Table 1 shows a comparison of the NSFD and Euler–Maruyama numerical schemes for the stochastic diabetes model. A few structural flaws limit the real-world accuracy of the proposed stochastic framework, even though it provides useful information about the dynamics of the diabetic community. First, it treats the population as uniformly mixed, which means local differences in healthcare access and regional disease patterns are not captured. Second, although the recruitment rate κ was held constant, it actually varies over time due to changes in screening regulations, migration, and birth rates. Third, the current formulation excludes age-structured progression, even though the clinical data suggest that progression and mortality risks ($\varpi_1, \varpi_2, \varpi_3, \theta$) vary significantly between young and senior cohorts. By filling in these gaps, the model's epidemiological accuracy would improve.

Table 1. Comparison of the NSFD and Euler–Maruyama (EM) numerical schemes for the stochastic diabetes model.

Property	**NSFD Scheme (Equations (21)–(23))**	**EM Scheme (Equations (18)–(20))**
Time-step restriction	The scheme remains stable and positivity-preserving, even for large $\Delta\tau$ (e.g., $\Delta\tau = 1$ day).	If the time steps are large, the solution may diverge or produce non-physical negative state values.
Time efficiency	The NSFD simulation requires a shorter cumulative runtime.	Due to an enormous number of iterations, the cumulative runtime is higher.
Total number of steps	Just 2000 steps are needed to cover a long-term horizon.	The steps are increased to achieve the same horizon.
Stability and positivity	The NSFD scheme is unconditionally stable and shows convergent behavior.	EM is conditionally stable and shows divergent behavior.

4.2. Conclusions

We began with the premise that standard deterministic models cannot properly describe pre-diabetes and diabetes dynamics, as real populations constantly face random environmental variations. Because deterministic models alone are ill-equipped to capture these real-world fluctuations, we examined a stochastic model for pre-diabetes and diabetes, both with and without complications, to evaluate the associated impacts on social and economic well-being. Using a stochastic non-negative Lyapunov function, we established the existence, uniqueness, and positivity of the solutions. We also derived sufficient conditions for a unique ergodic stationary distribution, which helped identify key

parameters that can inform strategies to mitigate the disease burden. We then developed a stochastic NSFD numerical scheme for approximation and validated that the scheme is mean-square consistent for the proposed model. Additionally, the stochastic NSFD scheme consistently converged toward the endemic equilibrium of the underlying deterministic system. Through numerical simulations, we observed how the intensity of the environmental noise affects the disease dynamics across all compartments, confirming our theoretical results. From a practical standpoint, promoting a healthy diet, regular physical activity, obesity prevention, and smoking cessation can lead to substantial progress in controlling pre-diabetes and diabetes progression.

4.3. Future Work

In future work, the present framework will be expanded upon in three key directions closely tied to the model structure. First, because the progression rates ($\varpi_1, \varpi_2, \varpi_3$) and natural mortality (θ) vary significantly across demographics, we will stratify the pre-diabetic, uncomplicated diabetic, and complicated diabetic compartments (T, U, V) into age-structured cohorts. Second, to formulate cost-effective strategies for health planners, time-dependent optimal control mechanisms will be introduced, including $u_1(t)$ to modulate the recruitment rate κ through lifestyle interventions and $u_2(t)$ to suppress the complicated progression rate ϖ_2 via targeted treatment intensity. Third, to evaluate the impact of sudden public health shocks or policy disruptions on the stationary distribution and assess the reliability of the NSFD scheme under discontinuous stress, standard Gaussian noise terms (ϱ_i) will be replaced with Lévy jump-diffusion processes.

Author Contributions: Conceptualization, J.E.M.-D., N.A. and M.W.Y.; methodology, J. and G.M.; software, J. and G.M.; validation, J., G.M., J.E.M.-D., M.W.Y., N.A. and L.E.A.-H.; formal analysis, J. and G.M.; investigation, J., G.M., J.E.M.-D., M.W.Y., N.A. and L.E.A.-H.; writing—original draft preparation, J. and G.M.; writing—review and editing, J., G.M., J.E.M.-D., M.W.Y., N.A. and L.E.A.-H.; visualization, J. and G.M.; supervision, J.E.M.-D., M.W.Y., N.A. and L.E.A.-H.; project administration, J.E.M.-D., M.W.Y., N.A. and L.E.A.-H. All authors have read and agreed to the published version of the manuscript.

Funding: This research received no external funding.

Data Availability Statement: This study did not involve the creation or analysis of data.

Acknowledgments: Author L.E.A-H. would like to thank the Secretary of Science, Humanities, Technology and Innovation of Mexico (SECIHTI) and the University of Guadalajara for the financial support through grant 779584 and the program PROSNII, respectively.

Conflicts of Interest: The authors declare no conflicts of interest.

Appendix A. Proof of the Stationary Distribution

Proof. Theorem 2 can be proven by satisfying the conditions of Lemma 1. Initially, the diffusion matrix of System (5)–(7) is defined as

$$Q = \begin{bmatrix} \varrho_1^2 T^2 & 0 & 0 \\ 0 & \varrho_2^2 U^2 & 0 \\ 0 & 0 & \varrho_3^2 V^2 \end{bmatrix}.$$

Additionally, if we set $S = \min_{(T,U,V)\in \bar{I}\subset \Re_+^3} \{\varrho_1^2 T^2, \varrho_2^2 U^2, \varrho_3^2 V^2\}$, then we formulate

$$\begin{aligned} \sum_{l,m=1}^{3} q_{lm}(T,U,V)_{\alpha_l \alpha_m} &= \varrho_1^2 T^2 \alpha_l^2 + \varrho_2^2 U^2 \alpha_2^2 + \varrho_3^2 V^2 \alpha_3^2 \\ &\geq S|\alpha|^2, \end{aligned} \tag{A1}$$

here, $(T, U, V) \in \bar{I}, \alpha = (\alpha_1, \alpha_2, \alpha_3) \in \Re_+^3$. Hence, condition (*i*) of Lemma 1 is satisfied. Next, to verify condition (*ii*), we require a candidate Lyapunov function that enforces strict positivity across all subpopulations while ensuring that the differential generator $\mathcal{L}$ is negative-definite outside a compact set. A logarithmic barrier structure is particularly well-suited for this purpose because it not only vanishes at the endemic equilibrium (T^*, U^*, V^*), but it also creates an infinite potential barrier as any state variable approaches zero (strictly preventing non-physical negative values), and balances the drift terms to satisfy Has'minskii's criterion for an ergodic stationary distribution. Driven by these analytical requirements, we constructed the C^2 non-negative Lyapunov function $\aleph : \mathbb{R}_+^3 \to \mathbb{R}_+$ by

$$\aleph_1 = c_3\aleph_2 - (\ln T + \ln V) + T + U + V, \tag{A2}$$

where $c_1, c_2, c_3 > 0$ are constants that will be calculated later and

$$\aleph_2 = T + U + V - c_1 \ln T - c_2 \ln U. \tag{A3}$$

Obviously,

$$\liminf_{\Upsilon\to\infty,(T,U,v)\in\Re_+^3\setminus Z_\Upsilon} \aleph_1(T, U, V) = +\infty, \tag{A4}$$

here, $Z_\Upsilon = (\frac{1}{\Upsilon}, \Upsilon) \times (\frac{1}{\Upsilon}, \Upsilon) \times (\frac{1}{\Upsilon}, \Upsilon)$.

Now we will show this for $\aleph_1(T, U, V)$ $\exists \min(\aleph_1(T_0^*, U_0^*, V_0^*))$. For this, take partial derivatives of $\aleph_1(T, U, V)$ w.r.t. (T, U, V):

$$\frac{\partial\aleph_1(T, U, V)}{\partial T} = 1 + c_3 - \frac{1 + c_1c_3}{T},$$

$$\frac{\partial\aleph_1(T, U, V)}{\partial U} = 1 + c_3 - \frac{c_2c_3}{U},$$

$$\frac{\partial\aleph_1(T, U, V)}{\partial V} = 1 + c_3 - \frac{1}{V},$$

Then, $\exists$ is only one unique stagnation point that is

$$(T_0^*{*}, U_0^*{*}, V_0^*{*}) = \left(\frac{1 + c_1c_3}{1 + c_3}, \frac{c_2c_3}{1 + c_3}, \frac{1}{1 + c_3}\right),$$

Furthermore, the Hessian matrix of $\aleph_1(T, U, V)$ at $\aleph_1(T_0^*, U_0^*, V_0^*)$ is

$$H = \begin{bmatrix} \frac{1+c_1c_3}{(T_0^*)^2} & 0 & 0 \\ 0 & \frac{c_2c_3}{(U_0^*)^2} & 0 \\ 0 & 0 & \frac{1}{(V_0^*)^2} \end{bmatrix}.$$

Here, $\aleph_1(T_0^*, U_0^*, V_0^*) > 0$ so that $H > 0$. We can determine that $\aleph_1(T, U, V)$ has $\min(\aleph_1(T_0^*, U_0^*, V_0^*))$. From (A4), we state that $\aleph_1(T, U, V)$ has only one unique minimum point that lies in $\Re_+^3$.

Now we generate a C^2-Lyapunov function $\aleph : \Re_+^3 \to \Re_+$ as

$$\aleph^*(T, U, V) = \aleph_1(T, U, V) - \aleph_1(T_0^*, U_0^*, V_0^*). \tag{A5}$$

By means of the Itô property and System (5)–(7), we derive the following aggregation:

$$\begin{aligned} \text{Ł}\aleph_2 = &\left(1-\frac{c_1}{T}\right)\Big(\kappa-(\theta+\varpi_3+\varpi_1)T(t)\Big)\\ &+\left(1-\frac{c_2}{U}\right)\Big(\varpi_1 T(t)-(\theta+\varpi_2)U(t)+\zeta V(t)\Big)\\ &+\Big(1\Big)\Big(\varpi_3 T(t)+\varpi_2 U(t)-(\theta+\zeta+\vartheta+\psi)V(t)\Big)\\ &\frac{c_1\varrho_1^2+c_2\varrho_2^2}{2}, \end{aligned} \tag{A6}$$

$$\begin{aligned} \text{Ł}\aleph_2 = \kappa-\theta\Big(T+U+V\Big)+c_1(\theta+\varpi_3+\varpi_1+\frac{\varrho_1^2}{2})\\ +c_2(\theta+\varpi_2+\frac{\varrho_2^2}{2})-\frac{c_1\kappa}{T}-(\vartheta+\psi)V-\frac{c_2}{U}(\varpi_1 T+\zeta V). \end{aligned}$$

On the localized compact domain I, let $U_{\max}=\sup_{(T,U,V)\in I} U<\infty$. Then, $1/U\geq 1/U_{\max}$, and hence,

$$-\frac{c_2}{U}(\varpi_1 T+\zeta V)\leq -\frac{c_2}{U_{\max}}(\varpi_1 T+\zeta V).$$

Consequently, the negative contribution is retained with the correct inequality direction. Applying the AM–GM inequality to the positive terms $\theta\Big(T+U+V\Big)=\theta(\frac{\kappa}{\theta})$, $\frac{c_1\kappa}{T}$ and $\frac{c_2\varpi_1 T}{U_{\max}}$ yields

$$-\kappa-\frac{c_1\kappa}{T}-\frac{c_2\varpi_1 T}{U_{\max}}\leq -3\left(\frac{c_1c_2\varpi_1\kappa^2}{U_{\max}}\right)^{1/3}.$$

Substitution into the preceding generator estimate gives the following localized upper bound:

$$\begin{aligned} \text{Ł}\aleph_2\leq \kappa+c_1\left(\theta+\varpi_3+\varpi_1+\frac{\varrho_1^2}{2}\right)+c_2\left(\theta+\varpi_2+\frac{\varrho_2^2}{2}\right)\\ -3\left(\frac{c_1c_2\varpi_1\kappa^2}{U_{\max}}\right)^{1/3}-(\vartheta+\psi)V-\frac{c_2\zeta}{U_{\max}}V. \end{aligned} \tag{A7}$$

Assume

$$c_1(\theta+\varpi_3+\varpi_1+\frac{\varrho_1^2}{2})=c_2(\theta+\varpi_2+\frac{\varrho_2^2}{2})=\kappa,$$

that is,

$$c_1=\frac{\kappa}{\theta+\varpi_3+\varpi_1+\frac{\varrho_1^2}{2}},$$

$$c_2=\frac{\kappa}{\theta+\varpi_2+\frac{\varrho_2^2}{2}}.$$

This implies the localized estimate

$$\text{Ł}\aleph_2\leq 3\kappa-3\left(\frac{c_1c_2\varpi_1\kappa^2}{U_{\max}}\right)^{1/3}-(\vartheta+\psi)V-\frac{c_2\zeta}{U_{\max}}V. \tag{A8}$$

Therefore, we formulated

$$Ł\aleph^* \leq c_3c_4 + \kappa - \frac{\kappa}{T} - \frac{\varpi_3 T}{V} - \frac{\varpi_2 U}{V} - \theta(T+U+V) - \zeta - \vartheta - \psi + \frac{\varrho_1^2 + \varrho_3^2}{2}, \tag{A9}$$

where $C_4 = -3\kappa\left[(\bar{R}_1^T)^{\frac{1}{3}} - 1\right] > 0$. Thereafter, define

$$I = \{\sigma_1 < T < \frac{1}{\sigma_4}, \sigma_2 < U < \frac{1}{\sigma_5}, \sigma_3 < V < \frac{1}{\sigma_6}\},$$

where $\sigma_i > 0 (i = 1,2,3,4,5,6)$ are moderately small constants. Now we divide the $\Re_+^3 \setminus I$ into the following six regions:

$$I_1 = \{(T,U,V) \in \Re_+^3, 0 < T \leq \sigma_1\},$$

$$I_2 = \{(T,U,V) \in \Re_+^3, 0 < U \leq \sigma_2, V > \sigma_1\},$$

$$I_3 = \{(T,U,V) \in \Re_+^3, 0 < V \leq \sigma_3, T > \sigma_2\},$$

$$I_4 = \{(T,U,V) \in \Re_+^3, 0 < T \geq \frac{1}{\sigma_4}\},$$

$$I_5 = \{(T,U,V) \in \Re_+^3, 0 < U \geq \frac{1}{\sigma_5}\},$$

$$I_6 = \{(T,U,V) \in \Re_+^3, 0 < V \geq \frac{1}{\sigma_6}\}.$$

In the stated set $\Re_+^3 \setminus I$, we can select the moderately small $\sigma_i > 0 (i = 1,2,3,4,5,6)$ such that the following conditions are satisfied:

$$\sigma_1^2 = \sigma_2, (\sigma_2)^3 = \sigma_3, -\frac{\kappa}{\sigma_1} + \bar{\Bbbk} < 0, -\frac{\varpi_2\sigma_2}{\sigma_1} + \bar{\Bbbk} < 0, -\frac{\varpi_3\sigma_2}{\sigma_3} + \bar{\Bbbk} < 0,$$
$$-\frac{\theta}{\sigma_4} + \bar{\Bbbk} < 0, -\frac{\theta}{\sigma_5} + \bar{\Bbbk} < 0, -\frac{\theta}{\sigma_6} + \bar{\Bbbk} < 0,$$

where $\bar{\Bbbk} > 0$ is constant. Moveover, we will show that $Ł\aleph^*(T,U,V) < 0$ in $\Re_+^3 \setminus I$.

(i) If $(T,U,V) \in I_1$, then, by (A9), we can acquire

$$Ł\aleph^* \leq c_3c_4 + \kappa - \frac{\kappa}{T} - \frac{\varpi_3 T}{V} - \frac{\varpi_2 U}{V} - \theta(T+U+V) - \zeta - \vartheta - \psi + \frac{\varrho_1^2 + \varrho_3^2}{2},$$

$$Ł\aleph^* \leq c_3c_4 + \kappa - \frac{\kappa}{T} - \zeta - \vartheta - \psi + \frac{\varrho_1^2 + \varrho_3^2}{2},$$

$$\leq c_3c_4 + \kappa - \zeta - \vartheta - \psi + \frac{\varrho_1^2 + \varrho_3^2}{2} - \frac{\kappa}{\sigma_1},$$

$$Ł\aleph^* \leq -\frac{\kappa}{\sigma_1} + \bar{\Bbbk}.$$

where

$$\bar{\Bbbk} = \sup_{(T,U,V)\in\Re_+^3} \left\{ c_3c_4 + \kappa - \frac{\kappa}{T} - \zeta - \vartheta - \psi + \frac{\varrho_1^2 + \varrho_3^2}{2}, \right.$$
$$\left. \leq c_3c_4 + \kappa - \zeta - \vartheta - \psi + \frac{\varrho_1^2 + \varrho_3^2}{2} \right\}.$$

By selecting a small $\sigma_1 > 0$ such that $c_3c_4 + \kappa - \zeta - \vartheta - \psi + \frac{\varrho_1^2+\varrho_3^2}{2} - \frac{\kappa}{\sigma_1} \leq 0$, then we can determine that $Ł\aleph^* < 0 \forall (T, U, V) \in I_1$.

(*ii*) If $(T, U, V) \in I_2$, then, by (A9), we can acquire

$$Ł\aleph^* \leq c_3c_4 + \kappa - \frac{\kappa}{T} - \frac{\varpi_3 T}{V} - \frac{\varpi_2 U}{V} - \theta(T + U + V) - \zeta - \vartheta - \psi + \frac{\varrho_1^2 + \varrho_3^2}{2},$$

$$Ł\aleph^* \leq c_3c_4 + \kappa - \frac{\varpi_2 U}{V} - \zeta - \vartheta - \psi + \frac{\varrho_1^2 + \varrho_3^2}{2},$$

$$\leq c_3c_4 + \kappa - \zeta - \vartheta - \psi + \frac{\varrho_1^2 + \varrho_3^2}{2} - \frac{\varpi_2\sigma_2}{\sigma_1},$$

$$Ł\aleph^* \leq -\frac{\varpi_2\sigma_2}{\sigma_1} + \bar{\mathbb{k}}.$$

By assuming that $\sigma_1^2 = \sigma_2$ and by selecting a possibly large enough $c_4 > 0$ and possibly small enough $\sigma_2 > 0$ such that $\leq c_3c_4 + \kappa - \zeta - \vartheta - \psi + \frac{\varrho_1^2+\varrho_3^2}{2} - \frac{\varrho_2\sigma_2}{\sigma_3} \leq 0$, then we can determine that $Ł\aleph^* < 0 \forall (T, U, V) \in I_2$.

(*iii*) If $(T, U, V) \in I_3$, then, by (A9), we can acquire

$$Ł\aleph^* \leq c_3c_4 + \kappa - \frac{\kappa}{T} - \frac{\varpi_3 T}{V} - \frac{\varpi_2 U}{V} - \theta(T + U + V) - \zeta - \vartheta - \psi + \frac{\varrho_1^2 + \varrho_3^2}{2},$$

$$Ł\aleph^* \leq c_3c_4 + \kappa - \frac{\varpi_3 T}{V} - \zeta - \vartheta - \psi + \frac{\varrho_1^2 + \varrho_3^2}{2},$$

$$\leq c_3c_4 + \kappa - \zeta - \vartheta - \psi + \frac{\varrho_1^2 + \varrho_3^2}{2} - \frac{\varpi_3\sigma_2}{\sigma_3},$$

$$Ł\aleph^* \leq -\frac{\varpi_3\sigma_2}{\sigma_3} + \bar{\mathbb{k}}.$$

Assume that $\sigma_2^3 = \sigma_3$ by selecting a possibly large enough $c_4 > 0$ and possibly small enough $\sigma_3 > 0$ such that $c_3c_4 + \kappa - \zeta - \vartheta - \psi + \frac{\varrho_1^2+\varrho_3^2}{2} - \frac{\varrho_3\sigma_1}{\sigma_2} \leq 0$; then, we can determine that $Ł\aleph^* < 0 \forall (T, U, V) \in I_2$.

(*iv*) If $(T, U, V) \in I_4$, then, by (A9), we can acquire

$$Ł\aleph^* \leq c_3c_4 + \kappa - \frac{\kappa}{T} - \frac{\varpi_3 T}{V} - \frac{\varpi_2 U}{V} - \theta(T + U + V) - \zeta - \vartheta - \psi + \frac{\varrho_1^2 + \varrho_3^2}{2},$$

$$Ł\aleph^* \leq c_3c_4 + \kappa - -\theta(T(t)) - \zeta - \vartheta - \psi + \frac{\varrho_1^2 + \varrho_3^2}{2},$$

$$\leq c_3c_4 + \kappa - \zeta - \vartheta - \psi + \frac{\varrho_1^2 + \varrho_3^2}{2} - \frac{\theta}{\sigma_4},$$

$$Ł\aleph^* \leq -\frac{\theta}{\sigma_4} + \bar{\mathbb{k}}.$$

By selecting a possibly small enough $\sigma_4 > 0$ such that $c_3c_4 + \kappa - \zeta - \vartheta - \psi + \frac{\varrho_1^2+\varrho_3^2}{2} - \frac{\theta}{\sigma_4} \leq 0$, then we can determine that $Ł\aleph^* < 0 \forall (T, U, V) \in I_4$.

(*v*) If $(T, U, V) \in I_5$, then, by (A9), we can acquire

$$Ł\aleph^* \leq c_3c_4 + \kappa - \frac{\kappa}{T} - \frac{\varpi_3 T}{V} - \frac{\varpi_2 U}{V} - \theta(T + U + V) - \zeta - \vartheta - \psi + \frac{\varrho_1^2 + \varrho_3^2}{2},$$

$$\text{Ł}\aleph^* \leq c_3c_4 + \kappa - \theta(U(t)) - \zeta - \vartheta - \psi + \frac{\varrho_1^2 + \varrho_3^2}{2},$$
$$\leq c_3c_4 + \kappa - \zeta - \vartheta - \psi + \frac{\varrho_1^2 + \varrho_3^2}{2} - \frac{\theta}{\sigma_5},$$
$$\text{Ł}\aleph^* \leq -\frac{\theta}{\sigma_5} + \bar{\mathbb{k}}.$$

By selecting a possibly small enough $\sigma_5 > 0$ such that $\leq c_3c_4 + \kappa - \zeta - \vartheta - \psi + \frac{\varrho_1^2+\varrho_3^2}{2} - \frac{\theta}{\sigma_5} \leq 0$, then we can determine that $\text{Ł}\aleph^* < 0 \forall (T, U, V) \in I_5$.

(*vi*) If $(T, U, V) \in I_6$, then, by (A9), we can acquire

$$\text{Ł}\aleph^* \leq c_3c_4 + \kappa - \frac{\kappa}{T} - \frac{\varpi_3 T}{V} - \frac{\varpi_2 U}{V} - \theta(T + U + V) - \zeta - \vartheta - \psi + \frac{\varrho_1^2 + \varrho_3^2}{2},$$
$$\text{Ł}\aleph^* \leq c_3c_4 + \kappa - \theta(V(t)) - \zeta - \vartheta - \psi + \frac{\varrho_1^2 + \varrho_3^2}{2},$$
$$\leq c_3c_4 + \kappa - \zeta - \vartheta - \psi + \frac{\varrho_1^2 + \varrho_3^2}{2} - \frac{\theta}{\sigma_6},$$
$$\text{Ł}\aleph^* \leq -\frac{\theta}{\sigma_6} + \bar{\mathbb{k}}.$$

By selecting a possibly small enough $\sigma_6 > 0$ such that $c_3c_4 + \kappa - \zeta - \vartheta - \psi + \frac{\varrho_1^2+\varrho_3^2}{2} - \frac{\theta}{\sigma_6} \leq 0$, then we can determine that $\text{Ł}\aleph < 0 \forall (T, U, V) \in I_6$. Eventually, we determine that $\text{Ł}\aleph^* < 0 \forall (T, U, V) \in I$, and hence, condition (*ii*) of Lemma 1 is satisfied. □

Appendix B. Proof of Stochastic Stability Analysis

Proof. The stochastic NSFD numerical scheme (21) for $T(t)$ is given by

$$T^{J+1} = \frac{T^J + \kappa\Delta\tau + \varrho_1 T^J(\chi_{1(J+1)\Delta\tau} - \chi_{1(J)\Delta\tau})}{1 + \Delta\tau(\theta + \varpi_3 + \varpi_1)},$$

where $\Delta\chi_{1J} = \chi_{1(J+1)\Delta\tau} - \chi_{1(J)\Delta\tau}$ is the increment in the Wiener process. The stability criteria are used for linear equations. So, the non-linear terms in (21) can be linearized by setting the local constant $\kappa = 0$. Thus,

$$T^{J+1} = \frac{T^J + \varrho_1 T^J \Delta\chi_{1J}}{1 + \Delta\tau(\theta + \varpi_3 + \varpi_1)}. \tag{A10}$$

Now, by taking the square of (A10) and then the expectations,

$$E[|T^{J+1}|^2] = E[|\frac{T^J + \varrho_1 T^J \Delta\chi_{1J}}{1 + \Delta\tau(\theta + \varpi_3 + \varpi_1)}|^2], \tag{A11}$$
$$E[|T^{J+1}|^2] = E[|T^J|^2|\frac{1 + \varrho_1\Delta\chi_{1J}}{1 + \Delta\tau(\theta + \varpi_3 + \varpi_1)}|^2].$$

Since T^J is independent of the future increment in the Wiener process $\Delta\chi_{1J}$, then

$$E[|T^{J+1}|^2] = E[|T^J|^2]E[|\frac{1 + \varrho_1\Delta\chi_{1J}}{1 + \Delta\tau(\theta + \varpi_3 + \varpi_1)}|^2], \tag{A12}$$
$$E[|T^{J+1}|^2] = E[|T^J|^2]E[|\frac{1}{1 + \Delta\tau(\theta + \varpi_3 + \varpi_1)}|^2|1 + \varrho_1\Delta\chi_{1J}|^2].$$

By utilizing the properties of the Wiener process increment,

$$E[|T^{J+1}|^2] = E[|T^J|^2](\frac{1}{1+\Delta\tau(\theta+\varpi_3+\varpi_1)})^2(1+\varrho_1^2\Delta t), \tag{A13}$$

The multiplying factor $(\frac{1}{1+\Delta\tau(\theta+\varpi_3+\varpi_1)})^2|(1+\varrho_1^2\Delta t)$ of $E[|T^J|^2]$ must be smaller than one in order to attain the stability condition, i.e.,

$$(\frac{1}{1+\Delta\tau(\theta+\varpi_3+\varpi_1)})^2(1+\varrho_1^2\Delta t) < 1,$$

By some simplification steps,

$$\varrho_1^2\Delta t - (\Delta t)^2(\theta+\varpi_3+\varpi_1)^2 - 2\Delta t(\theta+\varpi_3+\varpi_1) < 0,$$

As $\Delta t > 0$, the above equation can be written as

$$\varrho_1^2 - (\theta+\varpi_3+\varpi_1)[2+\Delta t(\theta+\varpi_3+\varpi_1)] \leq 0, \tag{A14}$$

As $\Delta t \to 0$, the numerical stability condition (A14) converges to the analytical stability condition. Therefore, the stochastic NSFD numerical scheme (21) for the exact solution of $T(t)$ is asymptotically stable in the mean square sense, that is, $\lim_{t\to\infty} E[|T(t)|^2]$ if, and only if, $\varrho_1^2 - 2(\theta+\varpi_3+\varpi_1) \leq 0$.

In the same way, we can establish the stability condition for $U(t)$. The stochastic NSFD numerical scheme (22) for $U(t)$ is given by

$$U^{J+1} = \frac{U^J + \Delta\tau(\varpi_1 T^J + \zeta V^J) + \varrho_2 U^J \Delta\chi_{2_J}}{1+\Delta\tau(\theta+\varpi_2)},$$

where $\Delta\chi_{2_J} = \chi_{2(J+1)\Delta\tau} - \chi_{2(J)\Delta\tau}$ is the increment in the Wiener process. The stability criteria were used for linear equations. So, the non-linear terms in (22) can be linearized by setting the $(T^J, V^J) = 0$. Thus,

$$U^{J+1} = \frac{U^J + \varrho_2 U^J \Delta\chi_{2_J}}{1+\Delta\tau(\theta+\varpi_2)}, \tag{A15}$$

Now, by taking the square of (A15) and then the expectations,

$$E[|U^{J+1}|^2] = E[|\frac{U^J + \varrho_2 U^J \Delta\chi_{2_J}}{1+\Delta\tau(\theta+\varpi_2)}|^2], \tag{A16}$$

$$E[|U^{J+1}|^2] = E[|U^J|^2|\frac{1+\varrho_2\Delta\chi_{2_J}}{1+\Delta\tau(\theta+\varpi_2)}|^2],$$

Since U^J is independent of the future increment in the Wiener process $\Delta\chi_{2_J}$, then

$$E[|U^{J+1}|^2] = E[|U^J|^2]E[|\frac{1+\varrho_1\Delta\chi_{2_J}}{1+\Delta\tau(\theta+\varpi_2)}|^2],$$

$$E[|U^{J+1}|^2] = E[|U^J|^2]E[|\frac{1}{1+\Delta\tau(\theta+\varpi_2)}|^2(1+\varrho_2\Delta\chi_{2_J}|^2],$$

By utilizing the properties of the Wiener process increment,

$$E[|U^{J+1}|^2] = E[|U^J|^2](\frac{1}{1+\Delta\tau(\theta+\varpi_2)})^2(1+\varrho_2^2\Delta t), \tag{A17}$$

The multiplying factor $(\frac{1}{1+\Delta\tau(\theta+\omega_2)})^2(1+\varrho_2^2\Delta t)$ of $E[|U^J|^2]$ must be smaller than one in order to attain the stability condition, i.e.,

$$(\frac{1}{1+\Delta\tau(\theta+\omega_2)})^2(1+\varrho_2^2\Delta t)<1, \tag{A18}$$

By some simplification steps,

$$\varrho_2^2\Delta t-(\Delta t)^2(\theta+\omega_2)^2-2\Delta t(\theta+\omega_2)<0,$$

As $\Delta t>0$, the above equation can be written as

$$\varrho_2^2-(\theta+\omega_2)[2+\Delta t(\theta+\omega_2)]\leq 0, \tag{A19}$$

As $\Delta t\to 0$, the numerical stability condition (A19) converges to the analytical stability condition. Therefore, the stochastic NSFD numerical scheme (22) for the exact solution of $T(t)$ is asymptotically stable in the mean square, that is, $\lim_{t\to\infty}E[|U(t)|^2]$ if, and only if, $\varrho_2^2-2(\theta+\omega_2)\leq 0$.

Similarly, we can establish the stability condition for $V(t)$. The stochastic NSFD numerical scheme (23) for $V(t)$ is given by

$$V^{J+1}=\frac{V^J+\Delta\tau(\omega_3T^J+\omega_2U^J)+\varrho_3V^J(\chi_{3(J+1)\Delta\tau}-\chi_{3(J)\Delta\tau})}{1+\Delta\tau(\theta+\zeta+\vartheta+\psi)}.$$

here, $\Delta\chi_{2J}=\chi_{2(J+1)\Delta\tau}-\chi_{2(J)\Delta\tau}$ is the increment in the Wiener process. The stability criteria are used for linear equations. So, the non-linear terms in (22) can be linearized by setting the $(T^J,V^J)=0$. Thus,

$$V^{J+1}=\frac{V^J+\varrho_3V^J\Delta\chi_{3J}}{1+\Delta\tau(\theta+\zeta+\vartheta+\psi)}, \tag{A20}$$

Now, by taking the square of (A20) and then the expectations,

$$E[|V^{J+1}|^2]=E[|\frac{V^J+\varrho_3V^J\Delta\chi_{3J}}{1+\Delta\tau(\theta+\zeta+\vartheta+\psi}|^2], \tag{A21}$$

$$E[|V^{J+1}|^2]=E[|V^J|^2|\frac{1+\varrho_3\Delta\chi_{3J}}{1+\Delta\tau(\theta+\zeta+\vartheta+\psi)}|^2],$$

Since U^J is independent of the future increment in the Wiener process $\Delta\chi_{2J}$, then

$$E[|V^{J+1}|^2]=E[|V^J|^2]E[|\frac{1+\varrho_3\Delta\chi_{3J}}{1+\Delta\tau(\theta+\zeta+\vartheta+\psi}|^2],$$

$$E[|V^{J+1}|^2]=E[|V^J|^2]E[|\frac{1}{1+\Delta\tau(\theta+\zeta+\vartheta+\psi)}|^2(1+\varrho_3\Delta\chi_{3J}|^2],$$

By utilizing properties of the Wiener process increment,

$$E[|V^{J+1}|^2]=E[|V^J|^2](\frac{1}{1+\Delta\tau(\theta+\zeta+\vartheta+\psi)})^2(1+\varrho_3^2\Delta t), \tag{A22}$$

The multiplying factor $(\frac{1}{1+\Delta\tau(\theta+\zeta+\vartheta+\psi)})^2(1+\varrho_3^2\Delta t)$ of $E[|V^J|^2]$ must be smaller than one in order to attain the stability condition, i.e.,

$$(\frac{1}{1+\Delta\tau(\theta+\zeta+\vartheta+\psi)})^2(1+\varrho_3^2\Delta t)<1, \tag{A23}$$

By some simplification steps,

$$\varrho_3^2\Delta t - (\Delta t)^2(\theta+\zeta+\vartheta+\psi)^2 - 2\Delta t(\theta+\zeta+\vartheta+\psi) < 0,$$

As $\Delta t > 0$, the above equation can be written as

$$\varrho_3^2 - (\theta+\zeta+\vartheta+\psi)[2+\Delta t(\theta+\zeta+\vartheta+\psi)] \leq 0, \tag{A24}$$

As $\Delta t \to 0$, then the numerical stability condition (A24) converges to the analytical stability condition. Therefore, the stochastic NSFD numerical scheme (22) for the exact solution of $T(t)$ is asymptotically stable in the mean square, that is, $\lim_{t\to\infty} E[|V(t)|^2]$ if, and only if, $\varrho_3^2 - 2(\theta+\zeta+\vartheta+\psi) \leq 0$. □

Appendix C. Proof of Stochastic Consistency Analysis

Proof. Suppose that $T(t)$ is a smooth function; then, by applying the operator $\mathcal{L}(G) = \int_{J\Delta\tau}^{(J+1)\Delta\tau} G_{(m)}dm$ to Equation (5), we formulated the following results:

$$\mathcal{L}(T)|_J = T_{((J+1)\Delta\tau)} - T_{(J\Delta\tau)} - \int_{J\Delta\tau}^{(J+1)\Delta\tau} \kappa dm + (\theta+\varpi_3+\varpi_1)\int_{J\Delta\tau}^{(J+1)\Delta\tau} T_{(m)}dm - \varrho_1\int_{J\Delta\tau}^{(J+1)\Delta\tau} T_{(m)}d\chi_{1(m)}, \tag{A25}$$

$$\mathcal{L}|_J(T) = T_{((J+1)\Delta\tau)} - T_{(J\Delta\tau)} - \Delta\tau\kappa + \Delta\tau(\theta+\varpi_3+\varpi_1)T_{(J\Delta\tau)} - \varrho_1 T_{(J\Delta\tau)}(\chi_1|^{(J+1)\Delta\tau} - \chi_1|^{J\Delta\tau}), \tag{A26}$$

$$\mathcal{L}(T)|_J - \mathcal{L}|_J(T) = (\theta+\varpi_3+\varpi_1)\int_{J\Delta\tau}^{(J+1)\Delta\tau}(T_{(m)} - T_{(J\Delta\tau)})dm + \varrho_1\int_{J\Delta\tau}^{(J+1)\Delta\tau}(-T_{(m)} + T_{(J\Delta\tau)})d\chi_{1(m)}. \tag{A27}$$

In the mean square,

$$E\left|\mathcal{L}(T)|_J - \mathcal{L}|_J(T)\right|^2 \leq 2E(\theta+\varpi_3+\varpi_1)^2\left|\int_{J\Delta\tau}^{(J+1)\Delta\tau}(T_{(m)} - T_{(J\Delta\tau))}dm\right|^2 + 2E\varrho_1^2\left|\int_{J\Delta\tau}^{(J+1)\Delta\tau}(-T_{(m)} + T_{(J\Delta\tau)}d\chi_1(m)\right|^2. \tag{A28}$$

By the square of the Itô integral property, that is,

$$E\left|\int_{p_o}^{p_1}\phi_{(\chi,m)}d\chi_m\right|^2 z \leq (p-p_o)^{z-1}z(2z-1)^z\int_{p_o}^{p_1}E\left|\phi_{(m,\chi)}\right|^2 zdm.$$

$$E\left|\mathcal{L}(T)|_J - \mathcal{L}|_J(T)\right|^2 \leq 2E(\theta+\varpi_3+\varpi_1)^2\left|\int_{J\Delta\tau}^{(J+1)\Delta\tau}(T_{(m)} - T_{(J\Delta\tau))}dm\right|^2 - 2E\varrho_1^2\int_{J\Delta\tau}^{(J+1)\Delta\tau}E\left|(-T_{(m)} + T_{(J\Delta\tau)}\right|^2 dm, \tag{A29}$$

$E\left|\mathcal{L}(T)|_J - \mathcal{L}|_J(T)\right|^2 \to 0$ as $\Delta\tau \to 0$. Hence, this scheme for T is consistent along the stochastic ODE (5). We will demonstrate the consistency of the scheme for U by using the same methodology. Suppose that $T(t)$, $U(t)$ and $V(t)$ are smooth functions; then,

by applying the operator $\mathcal{L}(G) = \int_{J\Delta\tau}^{(J+1)\Delta\tau} G_{(m)}dm$ to Equation (6), we formulated the following results:

$$\begin{aligned}\mathcal{L}(U)|_J = U_{((J+1)\Delta\tau)} - U_{(J\Delta\tau)} - \varpi_1 \int_{J\Delta\tau}^{(J+1)\Delta\tau} T_{(m)}dm \\ +(\theta+\varpi_2)\int_{J\Delta\tau}^{(J+1)\Delta\tau} U_{(m)}dm - \zeta\int_{J\Delta\tau}^{(J+1)\Delta\tau} V_{(m)}dm \\ -\varrho_2\int_{J\Delta\tau}^{(J+1)\Delta\tau} U_{(m)}d\chi_{2(m)},\end{aligned} \tag{A30}$$

$$\begin{aligned}\mathcal{L}|_J(U) = U_{((J+1)\Delta\tau)} - U_{(J\Delta\tau)} - \Delta\tau\varpi_1 T_{(J\Delta\tau)} + \Delta\tau(\theta+\varpi_2)U_{(J\Delta\tau)} \\ -\Delta\tau\zeta V_{(J\Delta\tau)} - \Delta\tau\varrho_2(\chi_2|^{(J+1)\Delta\tau} - \chi_2|^{J\Delta\tau}),\end{aligned} \tag{A31}$$

$$\begin{aligned}\mathcal{L}(U)|_J - \mathcal{L}|_J(U) = \varpi_1\int_{J\Delta\tau}^{(J+1)\Delta\tau}(-T_{(m)} + T_{(J\Delta\tau)})dm \\ +(\theta+\varpi_2)\int_{J\Delta\tau}^{(J+1)\Delta\tau}(U_{(m)} - U_{(J\Delta\tau)})dm + \zeta\int_{J\Delta\tau}^{(J+1)\Delta\tau}(-V_{(m)} + V_{(J\Delta\tau)})dm \\ +\varrho_2\int_{J\Delta\tau}^{(J+1)\Delta\tau}(-U_{(m)} + U_{(J\Delta\tau)})d\chi_{2(m)}.\end{aligned} \tag{A32}$$

In the mean square,

$$\begin{aligned}E\left|\mathcal{L}(U)|_J - \mathcal{L}|_J(U)\right|^2 = 4E\varpi_1^2\left|\int_{J\Delta\tau}^{(J+1)\Delta\tau}(-T_{(m)} + T_{(J\Delta\tau)})dm\right|^2 \\ +4E(\theta+\varpi_2)^2\left|\int_{J\Delta\tau}^{(J+1)\Delta\tau}(U_{(m)} - U_{(J\Delta\tau)})dm\right|^2 + 4E\zeta^2\left|\int_{J\Delta\tau}^{(J+1)\Delta\tau}(-V_{(m)} + V_{(J\Delta\tau)})dm\right|^2 \\ +4E\varrho_2^2\left|\int_{J\Delta\tau}^{(J+1)\Delta\tau}(-U_{(m)} + U_{(J\Delta\tau)})d\chi_{2(m)}\right|^2.\end{aligned} \tag{A33}$$

By the square of the Itô integral property, we conclude the following result:

$$\begin{aligned}E\left|\mathcal{L}(U)|_J - \mathcal{L}|_J(U)\right|^2 = 4E\varpi_1^2\left|\int_{J\Delta\tau}^{(J+1)\Delta\tau}(-T_{(m)} + T_{(J\Delta\tau)})dm\right|^2 \\ +4E(\theta+\varpi_2)^2\left|\int_{J\Delta\tau}^{(J+1)\Delta\tau}(U_{(m)} - U_{(J\Delta\tau)})dm\right|^2 + 4E\zeta^2\left|\int_{J\Delta\tau}^{(J+1)\Delta\tau}(-V_{(m)} + V_{(J\Delta\tau)})dm\right|^2 \\ +4\varrho_2^2\int_{J\Delta\tau}^{(J+1)\Delta\tau} E\left|(-U_{(m)} + U_{(J\Delta\tau)})\right|^2 dm.\end{aligned} \tag{A34}$$

$E\left|\mathcal{L}(U)|_J - \mathcal{L}|_J(U)\right|^2 \to 0$ as $\Delta\tau \to 0$. Hence, this scheme for U is consistent along the stochastic ODE (6). We will demonstrate the consistency of the scheme for V by using the same methodology. Suppose that $T(t)$, $U(t)$ and $V(t)$ are smooth functions; then, by applying the operator $\mathcal{L}(G) = \int_{J\Delta\tau}^{(J+1)\Delta\tau} G_{(m)}dm$ to Equation (7), we formulated the following results:

$$\mathcal{L}(V)|_J = V_{((J+1)\Delta\tau)} - V_{(J\Delta\tau)} - \omega_3 \int_{J\Delta\tau}^{(J+1)\Delta\tau} T_{(m)}dm - \omega_2 \int_{J\Delta\tau}^{(J+1)\Delta\tau} U_{(m)}dm + (\theta+\zeta+\vartheta+\psi)\int_{J\Delta\tau}^{(J+1)\Delta\tau} V_{(m)}dm - \varrho_3 \int_{J\Delta\tau}^{(J+1)\Delta\tau} V_{(m)}d\chi_{3(m)}, \tag{A35}$$

$$\mathcal{L}|_J(V) = V_{((J+1)\Delta\tau)} - V_{(J\Delta\tau)} - \Delta\tau\omega_3 T_{(J\Delta\tau)} - \Delta\tau\omega_2 U_{(J\Delta\tau)} + \Delta\tau(\theta+\zeta+\vartheta+\psi)V_{(J\Delta\tau)} - \Delta\tau\varrho_3(\chi_3|^{(J+1)\Delta\tau} - \chi_3|^{J\Delta\tau}), \tag{A36}$$

$$\mathcal{L}(V)|_J - \mathcal{L}|_J(V) = \omega_3 \int_{J\Delta\tau}^{(J+1)\Delta\tau}(-T_{(m)} + T_{(J\Delta\tau)})dm + \omega_2 \int_{J\Delta\tau}^{(J+1)\Delta\tau}(-U_{(m)} + U_{(J\Delta\tau)})dm + (\theta+\zeta+\vartheta+\psi)\int_{J\Delta\tau}^{(J+1)\Delta\tau}(V_{(m)} - V_{(J\Delta\tau)})dm + \varrho_3 \int_{J\Delta\tau}^{(J+1)\Delta\tau}(-V_{(m)} + V_{(J\Delta\tau)})d\chi_{3(m)}. \tag{A37}$$

In the mean square,

$$E\left|\mathcal{L}(V)|_J - \mathcal{L}|_J(V)\right|^2 = 4E\omega_3^2\left|\int_{J\Delta\tau}^{(J+1)\Delta\tau}(-T_{(m)} + T_{(J\Delta\tau)})dm\right|^2 + 4E\omega_2^2\left|\int_{J\Delta\tau}^{(J+1)\Delta\tau}(-U_{(m)} + U_{(J\Delta\tau)})dm\right|^2 + 4E(\theta+\zeta+\vartheta+\psi)^2\left|\int_{J\Delta\tau}^{(J+1)\Delta\tau}(V_{(m)} - V_{(J\Delta\tau)})dm\right|^2 + 4E\varrho_3^2\left|\int_{J\Delta\tau}^{(J+1)\Delta\tau}(-V_{(m)} + V_{(J\Delta\tau)})d\chi_{3(m)}\right|^2. \tag{A38}$$

By the square of the Itô integral property, we conclude the following result:

$$E\left|\mathcal{L}(V)|_J - \mathcal{L}|_J(V)\right|^2 \leq 4E\omega_3^2\left|\int_{J\Delta\tau}^{(J+1)\Delta\tau}(-T_{(m)} + T_{(J\Delta\tau)})dm\right|^2 + 4E\omega_2^2\left|\int_{J\Delta\tau}^{(J+1)\Delta\tau}(-U_{(m)} + U_{(J\Delta\tau)})dm\right|^2 + 4E(\theta+\zeta+\vartheta+\psi)^2\left|\int_{J\Delta\tau}^{(J+1)\Delta\tau}(V_{(m)} - V_{(J\Delta\tau)})dm\right|^2 + 4\varrho_3^2\int_{J\Delta\tau}^{(J+1)\Delta\tau} E\left|(-V_{(m)} + V_{(J\Delta\tau)})\right|^2 dm. \tag{A39}$$

$E\left|\mathcal{L}(V)|_J - \mathcal{L}|_J(V)\right|^2 \to 0$ as $\Delta\tau \to 0$. Hence, this scheme for V is consistent along the stochastic ODE (7). □

References

1. Acikgoz, S.U.; Diwekar, U.M. Blood glucose regulation with stochastic optimal control for insulin-dependent diabetic patients. *Chem. Eng. Sci.* **2010**, *65*, 1227–1236. [CrossRef]
2. Ahmad, E.; Lim, S.; Lamptey, R.; Webb, D.R.; Davies, M.J. Type 2 diabetes. *Lancet* **2022**, *400*, 1803–1820. [CrossRef] [PubMed]
3. Sayetta, R.B.; Murphy, R.S. Summary of current diabetes-related data from the National Center for Health Statistics. *Diabetes Care* **1979**, *2*, 105–119. [CrossRef] [PubMed]
4. Jacquez, J.A.; Simon, C.P. The stochastic SI model with recruitment and deaths I. Comparison with the closed SIS model. *Math. Biosci.* **1993**, *117*, 77–125. [CrossRef] [PubMed]
5. Cooper, I.; Mondal, A.; Antonopoulos, C.G. A SIR model assumption for the spread of COVID-19 in different communities. *Fractals* **2020**, *139*, 110057. [CrossRef] [PubMed]

6. Shi, H.; Duan, Z.; Chen, G. An SIS model with infective medium on complex networks. *Physica A Stat. Mech. Its Appl.* **2008**, *387*, 2133–2144. [CrossRef]
7. He, S.; Peng, Y.; Sun, K. SEIR modeling of the COVID-19 and its dynamics. *Nonlinear Dyn.* **2020**, *101*, 1667–1680. [CrossRef] [PubMed]
8. Dye, C.; Gay, N. Modeling the SARS epidemic. *Science* **2003**, *300*, 1884–1885. [CrossRef] [PubMed]
9. Ovaskainen, O.; Meerson, B. Stochastic models of population extinction. *Trends Ecol. Evol.* **2010**, *25*, 643–652. [CrossRef] [PubMed]
10. Khan, T.; Khan, A.; Zaman, G. The extinction and persistence of the stochastic hepatitis B epidemic model. *Fractals* **2018**, *108*, 123–128. [CrossRef]
11. Paliares, I.C.; Dualib, P.M.; Aroucha, P.M.T.; Torres, L.S.N.; de Sa, J.R.; Dib, S.A. Cardiovascular risk stratification in an ethnically mixed population with type 1 diabetes mellitus: Comparison of the steno type 1 risk engine with the Scottish-Swedish risk model. *Diabetes Res. Clin. Pract.* **2025**, *27*, 112386. [CrossRef] [PubMed]
12. Sibarani, M.H.; Wijaya, I.P.; Rizka, A.; Soewondo, P.; Riyadina, W.; Rahajeng, E.; Tahapary, D.L. Cardiovascular disease prediction model for Indonesian adult population with prediabetes and diabetes mellitus: The Bogor Cohort study of Noncommunicable Diseases Risk Factors. *Reviews* **2022**, *16*, 102330. [CrossRef] [PubMed]
13. Martínez-Hervás, S.; Morales-Suarez-Varela, M.M.; Andrés-Blasco, I.; Lara-Hernández, F.; Peraita-Costa, I.; Real, J.T.; Chaves, F.J. Developing a simple and practical decision model to predict the risk of incident type 2 diabetes among the general population: The di@bet.es study. *Eur. J. Intern. Med.* **2022**, *102*, 80–87. [CrossRef] [PubMed]
14. Winkley, K.; Graham, I.; Tylor, Y.; Chamley, M.; Rook, C.; Simpson, A.; Ismail, K. The psychosis and type 2 diabetes service model (PODS) population profile study. *Prim. Care Diabetes* **2025**, *19*, 329–333. [CrossRef] [PubMed]
15. Jones, A.P.; Homer, J.B.; Murphy, D.L.; Essien, J.D.; Milstein, B.; Seville, D.A. Understanding diabetes population dynamics through simulation modeling and experimentation. *Am. J. Public Health* **2006**, *96*, 488–494. [CrossRef] [PubMed]
16. Infante, S.; Hernández, A. Stochastic models to estimate population dynamics. *Inf. Comput.* **2019**, *7*, 311–328. [CrossRef]
17. Jagers, P. A general stochastic model for population development. *Scand. Actuar. J.* **1969**, *1969*, 84–103. [CrossRef]
18. Anusha, S.M.; Athithan, S. Dynamical Behaviour of a Stochastic Mathematical Model and Optimal Control for Type 2 Diabetes. *Math. Model. Eng. Probl.* **2024**, *11*, 792–798. [CrossRef]
19. Duun-Henriksen, A.K.; Schmidt, S.; Røge, R.M.; Møller, J.B.; Nørgaard, K.; Jørgensen, J.B.; Madsen, H. Model identification using stochastic differential equation grey-box models in diabetes. *J. Diabetes Sci. Technol.* **2013**, *7*, 431–440. Correction in *J. Diabetes Sci. Technol.* **2015**, *9*, 716. [CrossRef] [PubMed]
20. Zhang, Y.; Holt, T.A.; Khovanova, N. A data driven nonlinear stochastic model for blood glucose dynamics. *Comput. Methods Programs Biomed.* **2016**, *125*, 18–25. [CrossRef] [PubMed]
21. Slurink, I.A.; Kupper, N.; Smeets, T.; Soedamah-Muthu, S.S. Dairy consumption and risk of prediabetes and type 2 diabetes in the Fenland study. *Clin. Nutr.* **2024**, *43*, 69–79. [CrossRef] [PubMed]
22. Buysschaert, M.; Medina, J.L.; Bergman, M.; Shah, A.; Lonier, J. Prediabetes and associated disorders. *Endocrine* **2015**, *48*, 371–393. [CrossRef] [PubMed]
23. Schlesinger, S.; Neuenschwander, M.; Barbaresko, J.; Lang, A.; Maalmi, H.; Rathmann, W.; Herder, C. Prediabetes and risk of mortality, diabetes-related complications and comorbidities: Umbrella review of meta-analyses of prospective studies. *Diabetologia* **2022**, *65*, 275–285. [CrossRef] [PubMed]
24. Rooney, M.R.; Rawlings, A.M.; Pankow, J.S.; Tcheugui, J.B.E.; Coresh, J.; Sharrett, A.R.; Selvin, E. Risk of progression to diabetes among older adults with prediabetes. *JAMA Intern. Med.* **2021**, *181*, 511–519. Correction in *JAMA Intern. Med.* **2021**, *181*, 570. [CrossRef] [PubMed]
25. Khan, R.M.M.; Chua, Z.J.Y.; Tan, J.C.; Yang, Y.; Liao, Z.; Zhao, Y. From pre-diabetes to diabetes: Diagnosis, treatments and translational research. *Medicina* **2019**, *55*, 546. [CrossRef] [PubMed]
26. Cahn, A.; Shoshan, A.; Sagiv, T.; Yesharim, R.; Goshen, R.; Shalev, V.; Raz, I. Prediction of progression from pre-diabetes to diabetes: Development and validation of a machine learning model. *Diabetes/Metabolism Res. Rev.* **2020**, *36*, e3252. [CrossRef] [PubMed]
27. Khalaji, A.; Behnoush, A.H.; Saeedian, B.; Khanmohammadi, S.; Shokri Varniab, Z.; Peiman, S. Endocan in prediabetes, diabetes, and diabetes-related complications: A systematic review and meta-analysis. *Metab. Syndr.* **2023**, *15*, 102. [CrossRef] [PubMed]
28. Boutayeb, A.; Twizell, E.H.; Achouayb, K.; Chetouani, A. A mathematical model for the burden of diabetes and its complications. *Biomed. Eng. Online* **2004**, *3*, 20. [CrossRef] [PubMed]
29. Boutayeb, W.; Lamlili, M.E.; Boutayeb, A.; Derouich, M. A simulation model for the dynamics of a population of diabetics with and without complications using optimal control. In *International Conference on Bioinformatics and Biomedical Engineering*; Springer International Publishing: Cham, Switzerland, 2015; pp. 589–598.
30. Boutayeb, A.; Chetouani, A.; Achouyab, A.; Twizell, E.H. A non-linear population model of diabetes mellitus. *J. Appl. Math. Comput.* **2006**, *21*, 127–139. [CrossRef]
31. Boutayeb, A.; Chetouani, A. A population model of diabetes and pre-diabetes. *Int. J. Comput. Math.* **2007**, *84*, 57–66. [CrossRef]

32. Allen, E.J.; Allen, L.J.; Arciniega, A.; Greenwood, P.E. Construction of equivalent stochastic differential equation models. *Stoch. Anal. Appl.* **2008**, *26*, 274–297. [CrossRef]
33. Evans, L.C. *An Introduction to Stochastic Differential Equations*; American Mathematical Society: Providence, RI, USA, 2012; Volume 82.
34. Esquível, M.L.; Patrício, P.; Guerreiro, G.R. From ODE to Open Markov Chains, via SDE: An application to models for infections in individuals and populations. *Comput. Math. Biophys.* **2020**, *8*, 180–197. [CrossRef]
35. Smirnova, A.; DeCamp, L.; Chowell, G. Forecasting epidemics through nonparametric estimation of time-dependent transmission rates using the SEIR model. *Bull. Math. Biol.* **2019**, *81*, 4343–4365. [CrossRef] [PubMed]
36. Vinod, D.; Cherstvy, A.G.; Metzler, R.; Sokolov, I.M. Time-averaging and nonergodicity of reset geometric Brownian motion with drift. *Phys. Rev. E* **2022**, *106*, 034137. [CrossRef] [PubMed]
37. Wang, W.; Cherstvy, A.G.; Metzler, R.; Sokolov, I.M. Restoring ergodicity of stochastically reset anomalous-diffusion processes. *Phys. Rev. Res.* **2022**, *4*, 013161. [CrossRef]
38. Mao, X. *Stochastic Differential Equations and Applications*; Elsevier: Amsterdam, The Netherlands, 2007.
39. Din, A.; Khan, A.; Baleanu, D. Stationary distribution and extinction of stochastic coronavirus (COVID-19) epidemic model. *Fractals* **2020**, *139*, 110036. [CrossRef] [PubMed]
40. Li, Y.; Wei, Z. Dynamics and optimal control of a stochastic coronavirus (COVID-19) epidemic model with diffusion. *Nonlinear Dyn.* **2022**, *109*, 91–120. [CrossRef] [PubMed]
41. Wang, X.; Yasin, M.W.; Ahmed, N.; Rafiq, M.; Abbas, M. Numerical approximations of stochastic Gray–Scott model with two novel schemes. *Aims Math.* **2023**, *8*, 5124–5147. [CrossRef]
42. Yasin, M.W.; Ahmed, N.; Saeed, J.; Raza, A.; Rafiq, M.; Ahmad, H.; Almohsen, B. Numerical study of the reaction diffusion prey–predator model having Holling II Increasing Function in the predator under noisy environment. *J. Nonlinear Math. Phys.* **2024**, *31*, 68. [CrossRef]
43. World Health Organization. *Noncommunicable Diseases and Mental Health in Small Island Developing States*; World Health Organization: Geneva, Switzerland, 2023.
44. American Diabetes Association Professional Practice Committee for Diabetes. Introduction and methodology: Standards of Care in Diabetes-2026. *Diabetes Care* **2026**, *49*, S1–S5. [CrossRef] [PubMed]
45. Ong, K.L.; Stafford, L.K.; McLaughlin, S.A.; Boyko, E.J.; Vollset, S.E.; Smith, A.E.; Brauer, M. Global, regional, and national burden of diabetes from 1990 to 2021, with projections of prevalence to 2050: A systematic analysis for the Global Burden of Disease Study 2021. *Lancet* **2023**, *402*, 203–234. [CrossRef] [PubMed]
46. Tabák, A.G.; Herder, C.; Rathmann, W.; Brunner, E.J.; Kivimäki, M. Prediabetes: A high-risk state for developing diabetes. *Lancet* **2012**, *379*, 2279. [CrossRef] [PubMed]
47. Lean, M.E.; Leslie, W.S.; Barnes, A.C.; Brosnahan, N.; Thom, G.; McCombie, L.; Peters, C.; Zhyzhneuskaya, S.; Al-Mrabeh, A.; Hollingsworth, K.G.; et al. Primary care-led weight management for remission of type 2 diabetes (DiRECT): An open-label, cluster-randomised trial. *Lancet* **2018**, *391*, 541–551. [CrossRef] [PubMed]

Disclaimer/Publisher's Note: The statements, opinions and data contained in all publications are solely those of the individual author(s) and contributor(s) and not of MDPI and/or the editor(s). MDPI and/or the editor(s) disclaim responsibility for any injury to people or property resulting from any ideas, methods, instructions or products referred to in the content.